



Calhoun: The NPS Institutional Archive

Theses and Dissertations

Thesis Collection

1987

Mechanisms in thermal mechanical forming of plates.

Malaret, Hiram A.

<http://hdl.handle.net/10945/22833>

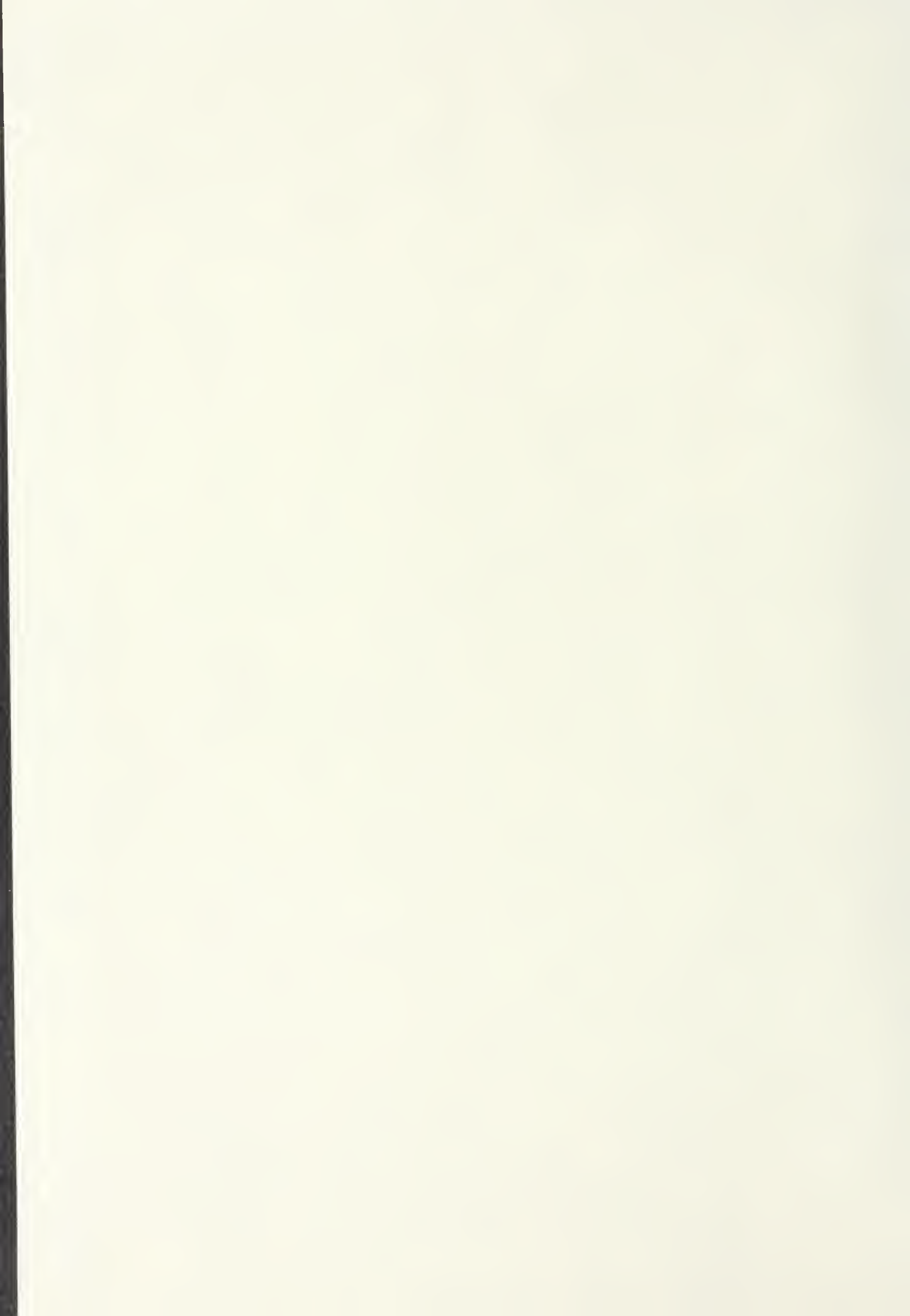


Calhoun is a project of the Dudley Knox Library at NPS, furthering the precepts and goals of open government and government transparency. All information contained herein has been approved for release by the NPS Public Affairs Officer.

Dudley Knox Library / Naval Postgraduate School
411 Dyer Road / 1 University Circle
Monterey, California USA 93943

<http://www.nps.edu/library>

LIBRARY
GRADUATE SCHOOL
CALIFORNIA 93943-6002



DEPARTMENT OF OCEAN ENGINEERING

MASSACHUSETTS INSTITUTE OF TECHNOLOGY

CAMBRIDGE, MASSACHUSETTS 02139

**MECHANISMS IN THERMAL
MECHANICAL FORMING OF PLATES**

by

Hiram A. Malaret

**S. M., NAME
S. M., ME**

**Course 13A
May 1987**

T234296

MECHANISMS IN THERMAL
MECHANICAL FORMING OF PLATES

by

Hiram A. Malaret

M.A., University of Miami
(1975)

Submitted to the Departments of Ocean Engineering and
Mechanical Engineering in partial fulfillment of the
requirements for the degrees of

S.M., Naval Architecture and Marine Engineering

and

S.M., Mechanical Engineering

at the

MASSACHUSETTS INSTITUTE OF TECHNOLOGY

May, 1987.

Massachusetts Institute of Technology

MECHANISMS IN THERMAL MECHANICAL FORMING OF PLATES

by

Hiram A. Malaret

Submitted to the Departments of Ocean Engineering and Mechanical Engineering on May, 1987 in partial fulfillment of the requirements for the degrees of S.M., Naval Architecture and Marine Engineering and S.M., Mechanical Engineering.

Abstract

The angular deflection produced by flame line heating as plate dimensions are varied, specifically in the direction of heating, is examined. The behavior is found to be similar to that observed when the line of heating approaches a plate edge and the bending, in both cases, can be obtained from the same parametric curve. The parameter values defining these curves are related to process variables: the thermal power and speed of travel of the heat source. Additionally, the in plate variation in bending is characterized.

The application of these findings to the formulation of a bending prediction model that incorporates plate dimensions as well as location of the heating line is presented. The extension of this model to predict bending at specific locations within the plate is discussed, and recommendations for further research are made.

ACKNOWLEDGEMENTS

I would like to express my gratitude to Professor Masubuchi for his support and guidance during the course of this investigation. My thanks also goes to Prof. A. Moshaiov and Visiting Engineer Akihiko Imakita, for their support. I would also like to thank LCDR William H. Luebke, USN for his cooperation. My thanks also goes to Mrs. Muriel Bernier.

To my sister Claudia for her assistance and patience in the typing of this thesis, my special thanks.

To my wife Lariana for her understanding and unfailing support especially during the past two years, my deepest gratitude.

The author hereby grants to MIT and to the United States Government and its agencies permission to reproduce and to distribute copies of this thesis in whole or in part.

TABLE OF CONTENTS

Abstract	2
Acknowledgements	3
1. INTRODUCTION	7
2. THERMO-MECHANICAL FORMING PROCESS	10
2.1 General Description	10
2.2 Factors Affecting Bending	14
2.3 Empirical vs. Theoretical	18
2.4 Specific Models	20
3. EXPERIMENTAL PROCEDURES	28
3.1 General Approach	28
3.2 Materials and Equipment	29
3.3 Experimental Setup	30
3.4 Procedures	32
4. EXPERIMENTAL RESULTS	37
4.1 General	37
4.2 Angular Deflection vs. Plate Length	38
4.3 Angular Deflection vs. In Plate Location	39
5. ANALYSIS	48
5.1 General	48
5.2 Angular Deflection vs. Plate Length	49
5.3 Angular Deflection vs. In Plate Location	54
6. CONCLUSIONS	69
References	73
Appendix	75

LIST OF FIGURES

- Figure 2.1** Temperature Dependent Properties: Yield Strength and Young's Modulus
- Figure 2.2** Temperature Dependent Properties: Coefficients of Strain Hardening and Thermal Expansion
- Figure 2.3** Temperature Dependent Properties: Yield Strain and Thermal Strain
- Figure 2.4** Effect of Location of Heat Source: Distance from Plate Edge vs. θ_c
- Figure 3.1** Experimental Setup for Line Heating
- Figure 3.2** Temperature Measurements: Location and Technique
- Figure 5.1** Addition of 3/8" Plate Flame Heating Data to Existing Parametric Curves
- Figure 5.2** Comparison of the Effect of Location of Heat Source with the Effect of Variation in Plate Length on Angular Deflection
- Figure 5.3** Angular Deflection Profile: Plate 8-4 After Cutting
- Figure 5.4** Angular Deflection Profile: Plate 1-3
- Figure 5.5** Angular Deflection Profile: Plate 1-4
- Figure 5.6** Angular Deflection Profile: Plate 1-5
- Figure 5.7** Angular Deflection Profile: Plate 1-6

LIST OF TABLES

Table 3.1	Plate Dimensions
Table 3.2	Plate Dimensions
Table 4.1	Temperature Measurements
Table 4.2	Angular Deflection by Plate-- Flame Heating
Table 4.3	Angular Deflection by Plate-- Laser Heating
Table 4.4	Pre-Heating Data and Calculated Angular Deflections-- Follow-on Experiment # 1
Table 4.5	Post-Heating Data and Calculated Angular Deflections-- Follow-on Experiment # 1
Table 4.6	Effect Due to Line Heating-- Follow-on Experiment # 1
Table 4.7	Effect of Sectioning Plate 0-4: First Through Third Cut
Table 4.8	Effect of Sectioning Plate 0-4: Fourth Through Seventh Cut
Table 5.1	Heat Deformation Model Predicted Deflections Compared to Experimental Results
Table 5.2	Results of Parametric Study

CHAPTER 1

INTRODUCTION

Industrial applications of metal plate forming processes are numerous. They range from forming the complex compound shapes of automobile body components to the various shapes required in the construction of ships and other marine structures.

The thin plate, high volume applications of the automobile industry are well suited to mechanical forming using press and die techniques. However, the thick plate low volume applications encountered in the shipbuilding and other large scale construction industries require other methods. The shaping of large, thick metal plate can be achieved by mechanical forming, thermo-mechanical forming, or some combination of the two. Mechanical forming of such large plate is limited to roller or break press methods, which are capable of producing curvature in one direction only, precluding the forming of complex shapes, such as in shell plating for a ship's bow or stern.

Thermo-mechanical methods, primarily that of line heating, have been used extensively for such shipbuilding applications for many years. In this technique, a heat source (usually an oxy-acetylene flame), is passed over the plate

surface to produce thermal stresses in the plate. These stresses in turn, cause yielding of the metal resulting in distortion of the plate. When implemented by highly skilled workers, who through years of practical experience have developed the art of determining how and where to apply the flame to produce desired shapes in a plate, the results are impressive. Compound shapes can be formed more rapidly and economically than by other methods, with less investment in capital equipment. However, the decreasing number of such highly skilled craftsmen in the work force, coupled with the continuing requirements of the shipbuilding industry, has emphasized a need for the development of new thermo-mechanical forming techniques that can be readily automated.

Toward this goal, the use of a laser heat source, with its increased stability and high power density, was proposed by Prof. Masubuchi. This resulted in the currently ongoing three year study, "*Laser Forming of Steel Plates for Ship Construction*," sponsored by the U. S. Navy and Todd Pacific Shipyards Corporation, under his direction. The first phase of this study included an investigation of primary and secondary factors influencing plate bending, the results of which are contained in the Phase I Report.^{'1'} Although the effects of plate thickness and location of the heat source

were examined, the effect of varying the plate dimensions was not.

The investigation of the effects associated with such changes in plate dimensions, particularly in the direction of movement of the heat source, is the basis of this thesis.

CHAPTER 2

THE THERMO-MECHANICAL FORMING PROCESS

2.1 General Description

In the thermo-mechanical forming process, the controlled application of heat is used to produce local thermal expansion, resulting in transient thermal stresses that exceed the yield strength of the material. This yielding produces local regions of plastic (non-elastic) strain which result in deformation and movement of the material as it returns to ambient temperature. The actual process is complex, as it involves the temperature dependent properties of the metal in the non-uniform temperature field produced by the heat source. Examples of this temperature dependence for a representative mild steel are illustrated in Figures 2.1 through 2.3 '4'. The stress-strain relationships, determined by three of these properties (yield strength, Young's modulus, and strain hardening), therefore exhibit corresponding changes with temperature. Any formal analysis of the mechanism must be able to address the formidable problem of accounting for these changes in properties and relationships with temperature at each point within the material. An excellent treatment is given in

"Theory of Thermal Stresses" by B. A. Boley and J. H. Weiner⁽⁷⁾; particularly Chapters 14 and 16, dealing with the formulation and analysis of the problem, respectively. However, for the current purpose, a less formal discussion similar to that given by McCarthy,⁽²⁾ is presented in the following paragraphs.

Fundamental to the forming process is the principal that plastic strain will occur only in the presence of some restraint that limits the thermal expansion of the material. As an illustration, consider the uniform heating of a totally unrestrained steel plate to just below its austenitizing temperature, A_1 , followed by uniform cooling to ambient temperature. Although the temperature exceeds that which would produce plastic yielding (flow) in a restrained plate, no deformation occurs. The uniform temperature field and the absence of any restraint allows the plate to expand and contract by the same amount during the thermal cycle. However, the presence of an external restraint or a sufficiently non-uniform temperature field will result in deformation.

The amount of plastic strain, produced whenever the thermal strain exceeds the yield strain of the material and defined as the difference of the two strains, represents the amount of deformation available at a given temperature. The

thermal strain produced is essentially the same for the various structural steels since the coefficient of thermal expansion exhibits slight change for these various steels. However, the yield strain, which is the quotient of the yield strength and Young's modulus of the material, varies significantly between the different steels. Thus, an upper limit to the amount of deformation that can be achieved by thermo-mechanical forming is established as a function of the yield strength of the material. It should be noted that due to the decrease of yield strength with increasing temperature, thermo-mechanical forming can produce bending with considerably lower and more uniform residual stress distributions, as compared to similar bending with direct mechanical forming methods as rolling or break press.

The most commonly practiced method of thermo-mechanical forming, as previously mentioned, is that of line heating in which no external restraint is applied. In this method, the heat source (usually an oxy-acetylene flame or laser) travels in a straight line along one axis of the plate. The restraint producing the plastic yielding is that of the cooler plate material surrounding that directly under the heat source. Thus, the temperature gradient in the plate has a significant effect on the amount of final

plate deformation produced. The mechanism can be qualitatively described as follows:

As the plate material under the heat source is heated beyond the point where plastic flow is initiated, this region of the plate will expand more rapidly than the cooler surrounding material, and will enter a state of compressive loading. The difference in loading through the thickness of the plate produces a moment that results in negative (concave down) deformation of the plate. As the heat source moves away, this region of the plate cools and the compressive plastic deformation that occurred in the upper portion of the plate produces a state of tension. The plate then rotates deforming positively (concave up) as it seeks to achieve equilibrium under this residual tensile stress. Since the resultant force and resultant moment produced by any residual stress must vanish, this implies that the residual tensile stress must be balanced by a compressive stress acting in the same section of the plate.

This description has served as the basis for various analytical models of the thermo-mechanical bending in plates. One such, the Heat Deformation model, developed by Iwasaki, et al ⁽⁵⁾, is used in the analysis of the results obtained during the current investigation, and will be discussed in more detail later in this chapter. Although the

above description of the thermo-mechanical process identified several major factors affecting the bending, there are other factors that contribute to the behavior. A summary of these factors is presented in the following section.

2.2 Factors Affecting Bending

The factors known to influence the bending process can be grouped according to their relative contribution to the overall behavior, as follows.

Primary Factors:

1. Yield Strength-- The higher the yield strength, implies that more thermal stress is required to produce yielding, resulting in less deformation or bending for a given heat input.
2. Heat Input-- The amount of deformation depends on both the maximum temperature obtained at a point during the heating and the temperature gradient in the vicinity of that point, particularly in the thickness direction. The heat input to the plate surface, usually expressed in terms of KJoules/inch, is primarily a function of the power produced by the heat source (KJoules /sec.) and the speed at which it moves over the plate. Another consideration of more consequence

in laser applications, is the coupling of the heat source to the plate. It should be noted that a higher heat input does not necessarily imply greater bending. If the power is too high or the speed too low, more material is heated to higher temperatures, and less restraint is available to produce plastic strain. Similarly, if the power is too low or the speed too high, the maximum temperature is decreased and less plastic strain produced. A parameter that has proved useful in relating the bending to the heat input is the power divided by the square root of the speed, P/\sqrt{V} .

3. Plate Thickness-- The dependence of the bending on the temperature gradient in the thickness direction would indicate that for each plate thickness there should exist some particular heat input that would optimize the bending. However, as the plate thickness increased, this heat input would also have to increase until one of two practical limits are reached: 1) the heat input would result in surface melting or 2) the plate would become so thick that the volume of material would prevent any motion, independent of the heat input.

Secondary factors:

1. Edge Restraint-- The plastic flow of the heated material is dependent on the restraint afforded by the surrounding cooler material. This can be augmented by the application of additional external restraint, such as clamping an edge of the plate. The closer the heat source is applied to the edge restraint, the more pronounced the bending.
2. Heating Location-- Relating to the discussion of the previous paragraph is the reduced bending obtained as the heat source is applied closer to a free edge. Actually, this observed "edge effect" is the consequence of two factors: the reduced material available to act as a heat sink both in the thickness direction as well as along the surface of the plate (resulting in a reduced temperature gradient), and the reduced mechanical restraint.
3. Applied Cooling-- Improvements in bending efficiency should be obtained if the temperature gradient in the thickness direction is increased. This can be achieved by forced cooling of the back side (side opposite the heat source) of the plate.
4. Geometric Constraint-- The bending produced by the heat source is affected by the plate geometry. If the

plate is already curved along an axis perpendicular to the line of heating, the moment of inertia would be greater than if the plate were flat. This effect influences the bending obtained when multiple passes at right angles to each other are used to produce a compound shape.

5. Pre-strain Condition-- If the plate has existing strain due to residual or imposed mechanical stresses prior to heating, its behavior will be modified. The presence of compressive strain will result in plastic flow occurring at lower temperatures (i.e. less thermal strain required for yielding). Conversely, the presence of tensile strain will raise the required thermal strain, raising the temperature required to initiate plastic flow. This is the primary cause for the reduced bending observed in successive passes of a heat source over the same line.

It is one of these secondary factors, namely that of heating location, that is central to the current investigation. The variations in bending behavior with plate length can be considered to be a direct consequence of this effect. The influence of these "edge effects" in large plates has been studied for the situation where the line of heating

is parallel to the edge in question.^{'1'} The effect on bending of varying the distance between a parallel edge and the line of heating is depicted in Figure 2.4. This behavior should be symmetrical with respect to the plate center with maximum bending occurring along the center line parallel to the edges considered. In this case, it is clear that decreasing edge to center line distance, as in a series of progressively narrower plates, will result in an accompanying decrease in bending. However, for the situation where the distance between the plate edges perpendicular to the line of heating is varied, the behavior could exhibit some difference from that previously discussed. Additionally, the bending produced at different locations along the line of heating could also differ, particularly near the edges. These possible differences being a consequence of the different orientation of the edges. An attempt to examine and if possible, to characterize this behavior motivated this investigation.

2.3 Empirical vs. Theoretical

The study of the behavior of plates subjected to transient thermal loading has produced several theoretical and numerical models that can predict the ultimate residual stress and strain distributions and resulting deformation.

The increasing capability and availability of computers has facilitated advances in the area of theoretical stress analysis. This has permitted the development of models, more capable of simulating the complex behavior of thermo-mechanical deformation. However, depending on the numerical methods used and approach taken, these models can be subject to several limitations. Some of these are practical i.e. computer time and cost required; others are analytic, i.e. the lack of an accurate thermo-elastic-plastic model that can simultaneously couple the thermal and mechanical effects. This last limitation results in the current practice of dividing the analysis into two parts: the thermal history (usually from experimental results) is established, and then served as input for the stress-strain analysis. A detailed discussion of this type of analysis, emphasizing the applications to the study of weld induced distortion, is found in Professor Masubuchi's *Analysis of Welded Structures*.⁽³⁾ It should be noted that in many practical applications, complete theoretical models are not required. The ultimate goal of the current research project, directed by Professor Masubuchi, i.e. the development of automated processes for the thermo-mechanical forming of steel plate, especially the high strength steels used in Naval applications is an example. Computer prediction models based on

experimentally determined empirical data can be used to control the automated process. Consequently, it appears that the most effective approach remains one of combined experimental work with theoretical stress analysis.

Part of the current effort is to determine parameters that will permit improved predictions when dealing with plates of varying dimensions.

2.4 Specific Models

In the course of this investigation, two models were considered for analysis of the experimental results and merit additional discussion. The following paragraphs outline the Heat Deformation Model presented by Iwasaki, et al ⁽⁵⁾, and the Elastic-Plastic Model presented by Iwamura and Rybicki. ⁽⁴⁾

Heat Deformation Model

The basic approach is that of considering the thermal transient to occur in a series of discrete steps in both space and time. This is accomplished by viewing the plate section at three time frames. The initial time frame is that of an unrestrained plate section of unit thickness at ambient temperature. The second time frame considers the plate section with the heat source directly above it and the

top surface at maximum temperature. At this point, the plate section is treated as if it consists of four regions: a top region of thickness n at a temperature T_h , a bottom region of thickness $1-n$ at a temperature T_r , and two side regions of unit thickness at ambient temperature that surround the heated regions. The values of n , T_h , and T_r are calculated using a model of the temperature field, and the plastic strain produced in the top region determined by the difference in the thermal strains experienced by the top and bottom regions less the yield strain of the material at T_h . The third time frame is that of the plate once again at ambient temperature, but now the compressive plastic strain formed during heating is producing tensile stress in the top region which is balanced by a compressive stress in the bottom region, resulting in bending. Application of equilibrium conditions and stress-strain relationships then provide an expression for the bending moment in terms of: the plastic strain produced, Young's modulus at ambient temperature, and the determined thickness of the T_h region, n . The predicted bending is then determined using the moment of inertia of the plate section and an effective width, w , also determined from the temperature field.

The procedure for determining n , T_h , T_r and w is fully discussed in the reference. But, it can be described as

follows: n is that distance from the top of the plate in which yielding is expected to occur at maximum temperature; T_n is the temperature at $n/2$; T_r is the bottom temperature when the top surface is at maximum temperature; $w/2$ is that distance from the center of the section where the temperatures at n and the plate bottom are such that yielding no longer occurs.

This model lends itself for very rapid real-time predictions of the bending performed on micro computers if provided with temperature inputs.

Inamura and Rybicki's Model

This two dimensional model considers the temperature dependent properties and includes elastic-plastic relations. Although incremental loading is used, the assumption of the stress paths for loading and unloading made by the authors results in a simplified set of stress-strain relations. The basic approach is to consider, for each load increment, that the total strain in the plate depends on the two dimensional variables, but in a linear manner with respect to each. The mechanical strain is taken as the difference between the total and thermal strain at each point. The total strain is estimated by applying equilibrium conditions for the stress through the plate thickness, where this stress is expressed in terms of the total and thermal strains. This provides

the computational algorithm with the iteration required to solve the resulting system of non-linear equations.

The displacement and deflection is then calculated for each load increment at each point in the grid representing the plate. The accumulated effects at the end of the thermal cycle are then used to calculate the residual strain and stress distributions predicted for the plate along with the distortion and deflection.

The predicted behavior is in very good agreement with the results of experiments performed by the authors using a very narrow, but thick metal plate.

An attempt to use this method to develop a computer model to serve as an analytic tool during the current investigation was undertaken. However, problems in convergence of the iterative procedure could not be overcome in time to support this objective.

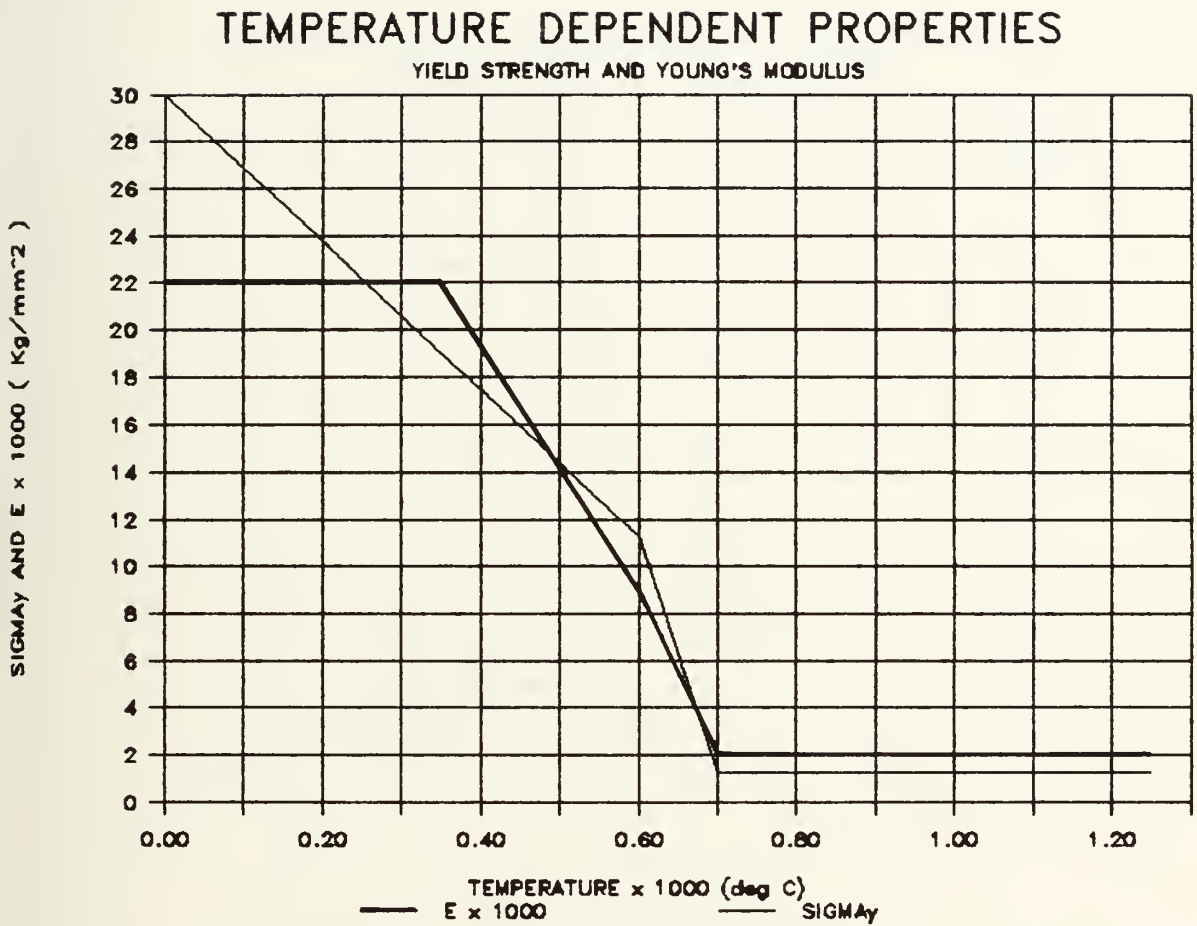


**FIGURE 2.1 TEMPERATURE DEPENDENT PROPERTIES:
YIELD STRENGTH AND YOUNG'S MODULUS**

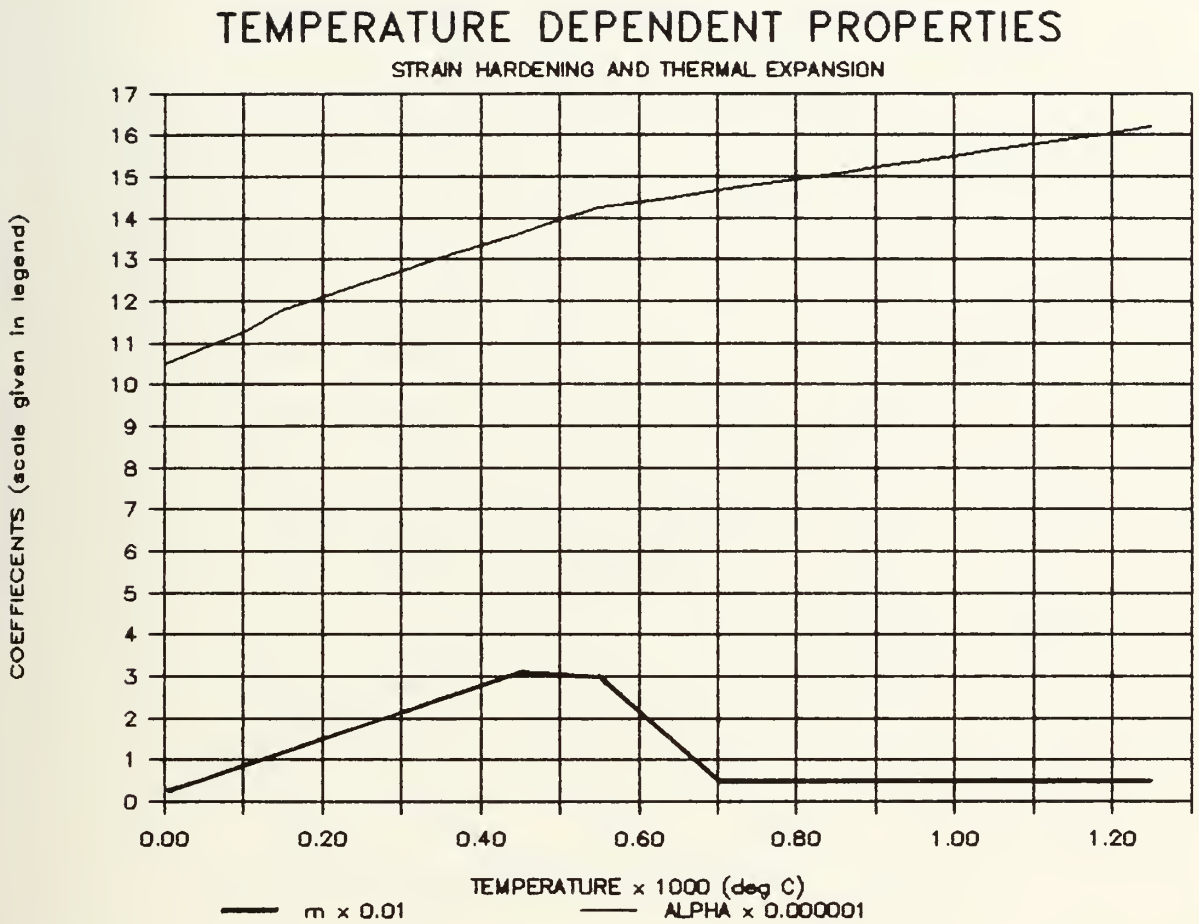


**FIGURE 2.2 TEMPERATURE DEPENDENT PROPERTIES:
COEFFICIENTS OF STRAIN HARDENING AND THERMAL EXPANSION**

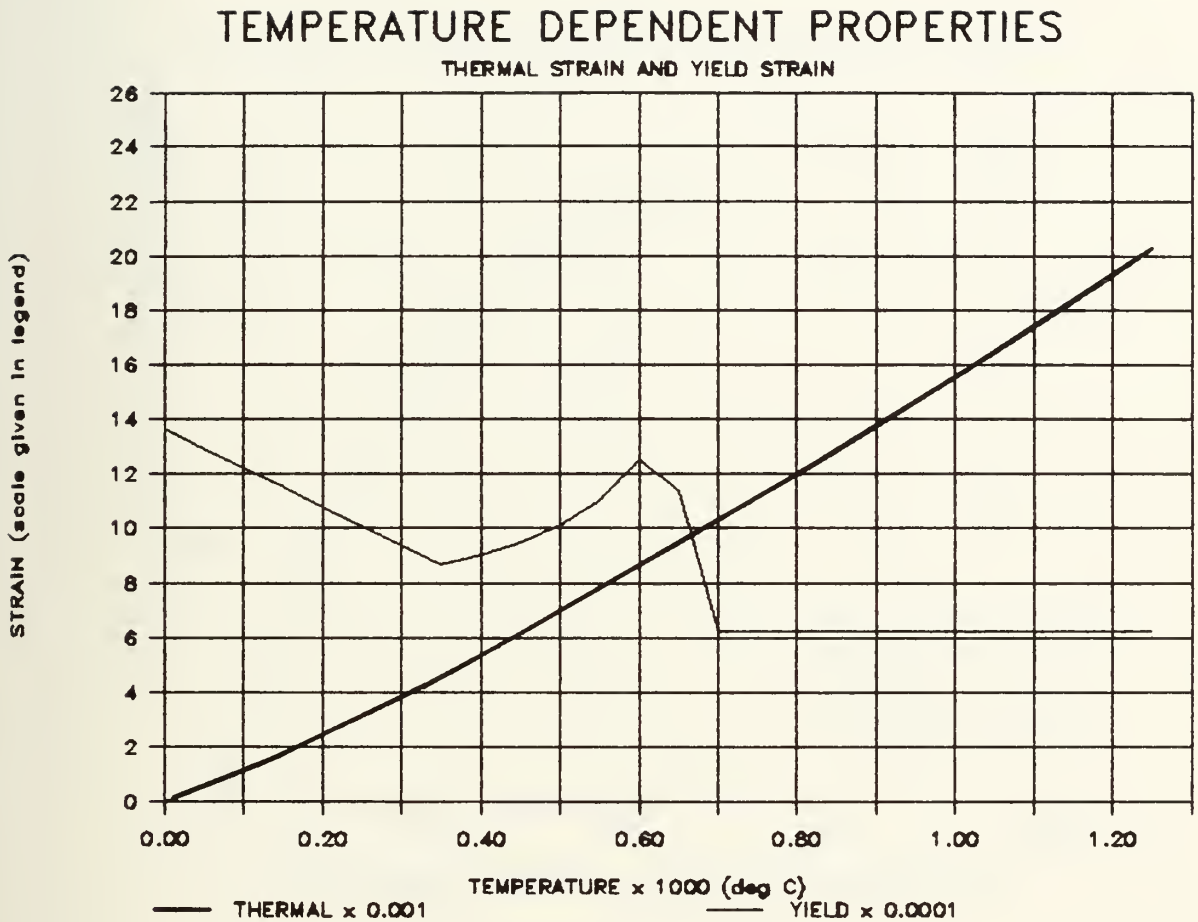


**FIGURE 2.3 TEMPERATURE DEPENDENT PROPERTIES:
YIELD STRAIN AND THERMAL STRAIN**

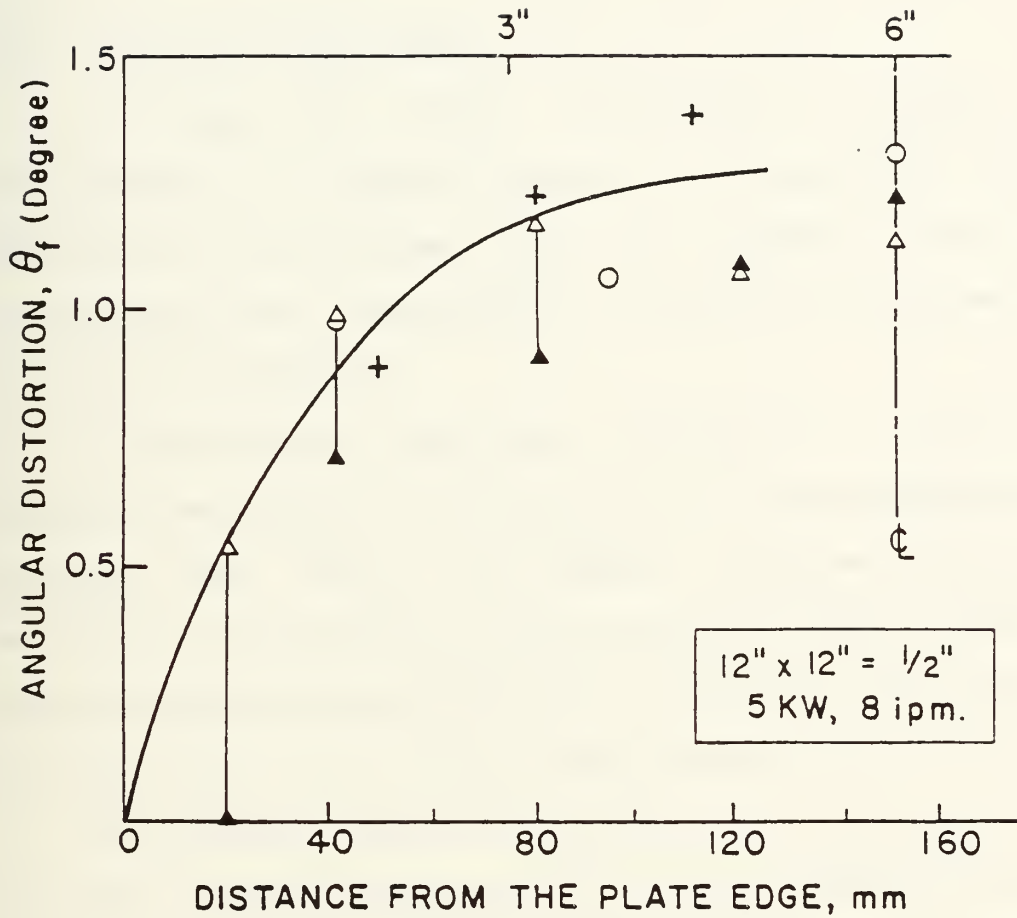


FIGURE 2.4 EFFECT OF LOCATION OF HEAT SOURCE:
DISTANCE FROM PLATE EDGE vs. θ_f

CHAPTER 3

EXPERIMENTAL PROCEDURES

3.1 General Approach

To study the overall dependence of plate bending (deflection) on length, plates of varying length but of the same width and thickness were line heated. The actual experiments were conducted in 3 parts as outlined in the following paragraphs.

A preliminary experiment, consisting of a series of 4 plates (designated 0-1 through 0-4), was conducted using a constant heat input. The results obtained indicated that subsequent experiments should include larger plates, and that as was expected, deflective behavior at the plate edges differed from that at the plate interior.

The largest plate of the series (12"x18"x3/8") was then cut into strips perpendicular to the direction of heating. The out-of-plane distortion after each cut, in the strips and the remaining plate, were recorded to provide data pertaining to the in plate deflective behavior noted.

Two follow-on experiments, each consisting of a series of 6 plates (designated 1-1 through 1-6 and 2-1 through 2-6), were then performed. One of these experiments was conducted at the same heat input as the preliminary

experiment; the other at a reduced heat input (approximately 1/2 that of the preliminary experiment). The heat input, expressed in terms of P/\sqrt{V} , was estimated from temperature measurements obtained for each experiment.

3.2 Materials and Equipment

The metal plate used in each of the experiments was Hot-rolled ASTM A-36 Low Carbon Steel plate. This material was not subjected to any special treatment. No attempts to remove any existing residual stresses from the rolling process were made. The surface preparation consisted only of cleaning and did not include any machining, other than grinding of the edges to remove metal burrs from the cutting of the plates to the required size by the supplier.

The dimensions of the plates used for each experiment are given in the Tables 3.1 and 3.2.

Commercially available oxy-acetylene torches were used for all of the experiments. The larger torch (an AIRCO type 800 with a #7 tip) produced average temperatures of 1000 degrees C and 506 degrees C at the top and bottom surfaces respectively. The other torch (a PUROX type W-200 with a #6 tip) produced average temperatures of 508 degrees C and 221 degrees C at the top and bottom surfaces respectively.

The temperature measurements were made with an unshielded 1/8" diameter K-type Chromal-Alumel thermocouple mounted at the end of a ceramic tube for support. The thermocouple was connected to an electronic ice point reference device, whose voltage output (in millivolts) was read on a digital voltmeter. This voltage data was then converted to the corresponding temperatures. The choice of the bead size was dictated by the need for a relatively small thermocouple time constant.

The mechanical dial indicator used for distortion measurements had a range of 3 inches with an accuracy of 0.0005 inch (i.e. direct reading to the nearest 0.001 inch).

3.3 Experimental Setups

In all the experiments, the plates were simply supported along lines parallel to the line of heating, and at a distance of one fourth the plate width (4.5 inches) from each edge. The torch was mounted to a variable speed electro-mechanical carriage, set at a speed of 7.5 in/min \pm 0.5 in/min, to move the flame over the plates at constant speed and torch tip height. This arrangement is illustrated in Figure 3.1.

To determine initial (pre-heating) and final (post-heating) plate distortion, a flat (granite) table was used

to support the plates, and the mechanical dial indicator affixed to a flat block, was used to measure the out of plane distortion of the plates.

The cutting of the one plate from the preliminary experiment was done on a band saw at slow speed to minimize the introduction of additional distortion due to local heating in the vicinity of the cutting line.

Temperature readings were taken at four locations on a representative plate for each of the two heat input levels used. These four locations were the top and bottom plate surfaces both at near edge (0.5 inches from the edge), and at the plate interior (5 inches from the edge). These measurements were obtained using the bead type thermocouple in contact with the plate surface. The top surface measurements were taken at a point 0.5 to 0.75 inches behind the moving torch with the thermocouple bead shielded from the deflected hot gases from the torch flame by a ceramic plate, as illustrated in Figure 3.2. However, with the larger torch, the increased volume of deflected gases made it difficult to obtain accurate readings, even with the ceramic shield. The bottom surface measurements were taken immediately after the tip passed the indicated location.

3.4 Procedures

Each experiment was carried out in three steps or procedures which are detailed in the following paragraphs.

Initial Measurement Procedure. This consisted of surface cleaning of each plate to be used in the experiment, followed by the marking of a reference grid on the top surface. Then initial out of plane distortion of each plate over its surface was measured using the flat table and mechanical dial indicator and the raw data recorded.

Line Heating Procedure. In preparation for the actual line heating, the plates were placed on the support structure. Alignment of the plates and leveling of the support structure to ensure consistency of torch tip position and height over all the plates, was then performed. Finally, torch travel speed was set and measured by operating the carriage. Then the actual line heating of the plates was performed. The average torch speed was again measured during the heating. The plates were then allowed to cool, in air, to room temperature.

Final Measurement Procedure. The out of plane distortion of the cooled plates was then determined in the same manner as described for the initial measurements and the raw data recorded.

The raw data, in the form of the relative out of plane distortion, was then converted to angular deflection along each grid line and an average angular deflection for each plate calculated. To accomplish this, a linear regression of the raw distortion readings versus distance from the line of heating along each grid line was performed. This resulted in two straight lines, each perpendicular to and extending from the line of heating to the corresponding edge. The angular deflection along each grid line was then calculated using the slopes of these two lines. This was done for the initial (pre-heating) and final (post-heating) distortion readings at each grid line. The actual heat induced bending of the plates along each grid line, expressed as angular deflection, was then taken as the difference of the final and initial angular deflections for that grid line.

For the preliminary experiment, the additional procedure of cutting of the larger plate (0-4, 12"x18"x3/8") into 1.5 inch strips about each grid line perpendicular to the line of heating was performed. After each cut, the relative out-of-plane distortion at points along the grid lines on the plate as well as the cut strip were measured. This raw data was then converted to angular deflections, as outlined in the previous paragraph.

Preliminary Experiment (4 plates)

PLATE #	DIMENSIONS
0-1	3"x18"x3/8"
0-2	6"x18"x3/8"
0-3	9"x18"x3/8"
0-4	12"x18"x3/8"

Table 3.1 Plate Dimensions

Follow-On Experiments (6 plates)

PLATE #	DIMENSIONS
1-1, 2-1	3"x18"x3/8"
1-2, 2-2	6"x18"x3/8"
1-3, 2-3	9"x18"x3/8"
1-4, 2-4	12"x18"x3/8"
1-5, 2-5*	15"x18"x3/8"
1-6, 2-6*	18"x18"x3/8"

* THESE FOUR WERE STAMPED OUT (PRESS CUT) FROM A LARGER PLATE, INSTEAD OF CUT FROM PLATES HOT-ROLLED TO THEIR RESPECTIVE LENGTHS, AS THE SMALLER PLATES IN THE SERIES.

Table 3.2 Plate Dimensions

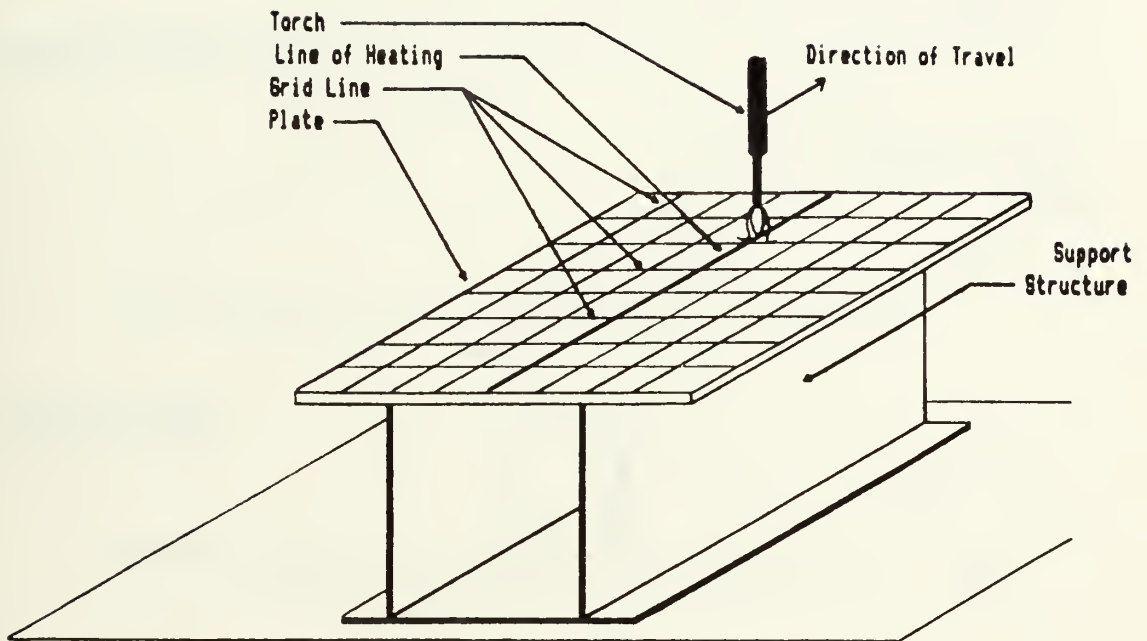


FIGURE 3.1 EXPERIMENTAL SETUP FOR LINE HEATING

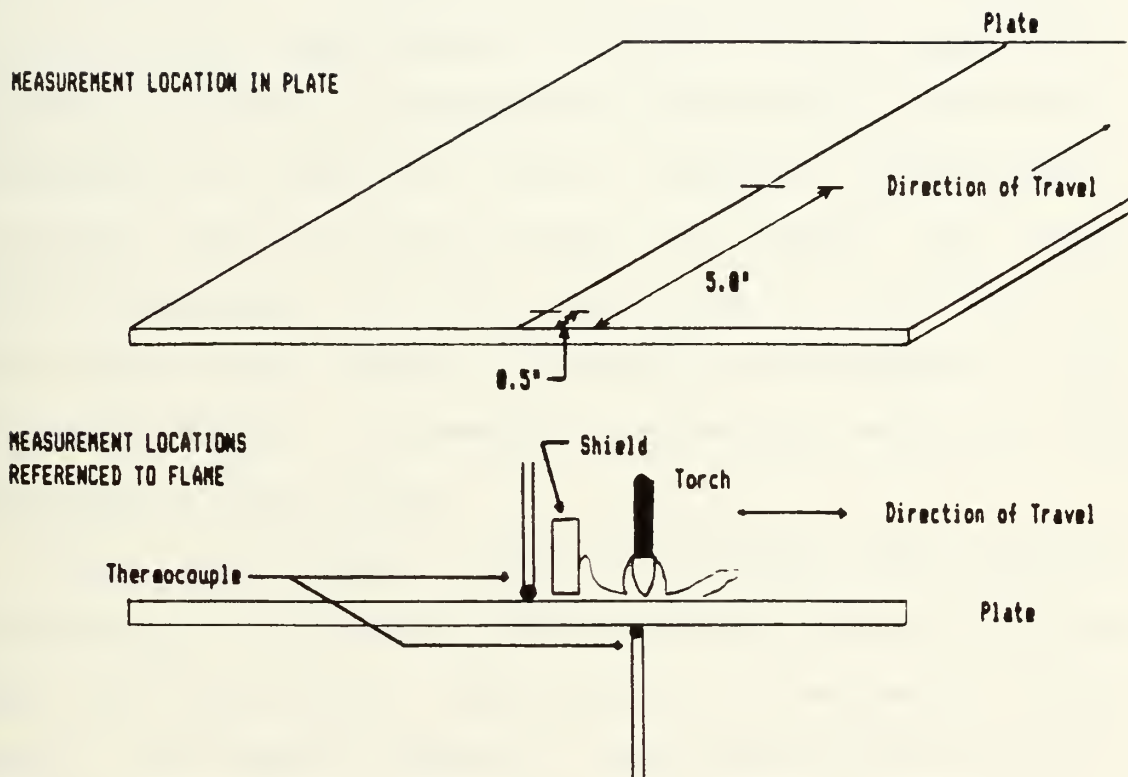


FIGURE 3.2 TEMPERATURE MEASUREMENTS: LOCATION AND TECHNIQUE

CHAPTER 4

EXPERIMENTAL RESULTS

4.1 General

The actual data obtained from the three experiments performed described the bending as a function of position at various points along the line of heating in each plate. This data could be used directly to examine the "edge effect" associated with the location of the heat source within each plate. However, to study the influence of plate dimensions (length) on bending, an average deflection was calculated for each plate.

These experimental results indicated that bending varied within the plate, generally being less at the plate edges, and that bending decreased with decreasing plate length. The results supporting these observations are presented and discussed in the remainder of this chapter.

Additionally, the results of the temperature measurements taken at the top and bottom surfaces of representative plates for each heat input, are presented in Table 4.1.

4.2 Angular deflection vs Plate length

The experimental results relating to this behavior are presented in Table 4.2, in which the angular deflections given represent plate averages. The general pattern observed in each case is the same, that of decreasing bending with decreasing plate length. The scatter exhibited by the data is attributed primarily to existing residual stress distributions in the plates themselves, which could differ widely from plate to plate. As commented in Table 3.2 of the previous chapter, Hot-rolled plates were used, to which different cutting and edging techniques were applied to the different plates by the commercial supplier.

To further increase the data available for analysis and to examine possible behavior variations with a different type of heat source and different plate thicknesses, LCDR W. H. Luebke graciously permitted measurements to be taken of plates line heated in experiments performed in the course of his investigation.⁶ These experiments were conducted using a variable power laser as the heat source, operated at power levels and travel speeds comparable to those used in the experiments presented in this thesis. Luebke's experiments examined the behavior of steel plates with thicknesses of 3/8", 1/2", and 5/8", and lengths of 1", 10", and 20".

In both cases, laser and flame line heating, the same width (18") plate was used. This data is summarized in Table 4.3.

The results obtained from both the flame and laser experiments served as basis for parametric studies performed in Chapter 5.

4.3 Angular Deflection vs. In Plate Location

The data used to determine the bending along each grid line for each plate of the first follow-on experiment, is fully detailed in Tables 4.4 through 4.6. Additionally, the data obtained in the cutting of the largest plate of the preliminary experiment is given in Tables 4.7 and 4.8. In both sets of data, the resulting angular deflections show variations in bending through the respective plates. However, the results of the follow-on experiment exhibit considerable scatter, particularly for the large plates, masking in part any general trends. To identify such trends, both a linear and quadratic least square fit was performed on the data for each plate; the results of which are presented and discussed in Chapter 5. The tabulated results for the cut plate, however, do provide a very clear pattern. The bending of the outer strips is definitely reduced, with an overall increase in bending between the strips when viewed in the same direction of travel as the

heat source. This reduced bending at the edges was expected from the discussion of secondary factors; however the overall increase in deflection along the length of the plate was not. This implied asymmetric behavior with respect to the plate center. A possible explanation of which is given in the next chapter. It is noted that the linear and quadratic least square fits result in curves presenting similar behavior to that of the cut plate in two of the four cases considered.

TORCH/TIP USED	PLATE LOCATION	THERMOCOUPLE READING (mV)	TEMPERATURE (deg C)
AIRCO TYPE 800	PLATE NEAR EDGE (0.5" FROM EDGE)		
# 7 TIP	TOP SURFACE	40.0*	1000.0*
	BOTTOM SURFACE	20.9	506.2
	PLATE INTERIOR (5.0" FROM EDGE)		
	TOP SURFACE	40.0*	1000.0*
	BOTTOM SURFACE	19.0	461.7
PURON TYPE W-200	PLATE NEAR EDGE: (0.5" FROM EDGE)		
# 6 TIP	TOP SURFACE	21.0	508.6
	BOTTOM SURFACE	9.0	221.3
	PLATE INTERIOR: (5.0" FROM EDGE)		
	TOP SURFACE	21.0	508.6
	BOTTOM SURFACE	8.5	209.0

* NOTE: THESE READINGS HAD TO BE ESTIMATED, APPROXIMATE TEMPERATURE DETERMINED WITH TEMP-STICK CRAYONS

TABLE 4.1 TEMPERATURE MEASUREMENTS

SUMMARY OF ANGULAR DEFLECTIONS OBTAINED BY FLAME LINE HEATING				SUMMARY OF ANGULAR DEFLECTIONS OBTAINED BY LASER LINE HEATING			
EXPERIMENT	PLATE #	DIMENSIONS	THETAT (Grads)	LASER POWER	P / \sqrt{V}	DIMENSIONS	THETAT (Grads)
PRELIMINARY	0-1	3" X 10" X 3/8"	0.0127	6 Kw	2.0	1" X 10" X 3/8"	0.0049
	0-2	6" X 18" X 3/8"	0.0179			18" X 10" X 3/8"	0.0037
	0-3	9" X 18" X 3/8"	0.0216			20" X 10" X 3/8"	0.0087
	0-4	12" X 18" X 3/8"	0.0248				
FOLLOW-ON # 1	1-1	3" X 18" X 3/8"	0.0045	6 Kw	2.5	1" X 10" X 3/8"	0.0028
	1-2	6" X 10" X 3/8"	0.0090			10" X 18" X 3/8"	0.0158
	1-3	9" X 10" X 3/8"	0.0092			20" X 10" X 3/8"	0.0178
	1-4	12" X 10" X 3/8"	0.0080				
	1-5	15" X 18" X 3/8"	0.0084	5 Kw	1.0	1" X 10" X 1/2"	0.0014
	1-6	18" X 18" X 3/8"	0.0090			18" X 18" X 1/2"	0.0147
FOLLOW-ON # 2	2-1	3" X 10" X 3/8"	0.0079	5 Kw	2.5	1" X 10" X 1/2"	0.0080
	2-2	6" X 10" X 3/8"	0.0219			10" X 10" X 1/2"	0.0324
	2-3	9" X 10" X 3/8"	0.0221			20" X 10" X 1/2"	0.0268
	2-4	12" X 10" X 3/8"	0.0390				
	2-5	15" X 10" X 3/8"	0.0334	0 Kw	3.0	1" X 10" X 5/8"	0.0032
	2-6	18" X 10" X 3/8"	0.0399			18" X 10" X 5/8"	0.0268
						20" X 10" X 5/8"	0.0324
				0 Kw	3.5	1" X 10" X 5/8"	0.0034
						18" X 10" X 5/8"	0.0262
						20" X 10" X 5/8"	0.0308

TABLE 4.2

ANGULAR DEFLECTIONS BY PLATE - FLAME HEATING

TABLE 4.3

ANGULAR DEFLECTIONS BY PLATE - LASER HEATING

PLATE #	GRID LINE #	DIMENSIONS	OUT OF PLANE DISTORTION					Y					ANGULAR DEFLECTION				
			1.5	3.0	6.0	9.0	12.0	15.0	18.0	A1	A2	THETA					
1-1	3" X 18" X 3/8"	1	1.5	0.000	0.004	0.007	0.003	-0.001	-0.002	0.000	0.004	-0.0003	-0.0007	0.000	0.000	0.000	0.000
			AVERAGE	0.000	0.004	0.007	0.003	-0.001	-0.002	0.000	0.004	-0.0003	-0.0007				
1-2	6" X 18" X 3/8"	1	1.5	-0.004	-0.043	-0.072	-0.067	-0.066	-0.032	0.000	-0.003	0.0008	0.0191	0.000	0.000	0.000	0.000
		2	3.0	0.000	-0.040	-0.068	-0.065	-0.066	-0.035	-0.000	-0.004	0.0007	0.0182				
		3	4.5	0.002	-0.039	-0.069	-0.067	-0.075	-0.043	-0.000	-0.009	0.0078	0.0177				
		AVERAGE	0.001	-0.041	-0.070	-0.066	-0.066	-0.069	-0.037	-0.000	-0.009	0.0008	0.0183				
1-3	9" X 18" X 3/8"	1	1.5	-0.043	-0.040	-0.047	-0.051	-0.048	-0.029	0.000	-0.010	0.0057	0.0068	0.000	0.000	0.000	0.000
		2	3.0	-0.034	-0.034	-0.041	-0.046	-0.041	-0.021	0.006	-0.014	0.0059	0.0073				
		3	4.5	-0.030	-0.032	-0.040	-0.045	-0.039	-0.015	0.011	-0.018	0.0064	0.0082				
		4	6.0	-0.034	-0.033	-0.042	-0.046	-0.039	-0.015	0.016	-0.015	0.0078	0.0085				
		5	7.5	-0.030	-0.037	-0.047	-0.050	-0.043	-0.014	0.016	-0.015	0.0076	0.0091				
		AVERAGE	0.036	-0.035	-0.043	-0.048	-0.042	-0.039	-0.019	0.010	-0.015	0.0065	0.0080				
1-4	12" X 18" X 3/8"	1	1.5	0.032	0.017	0.002	-0.007	-0.010	-0.007	0.000	-0.004	0.0008	0.0052	0.000	0.000	0.000	0.000
		2	3.0	0.033	0.022	0.006	-0.002	-0.004	0.000	0.000	-0.004	0.0011	0.0051				
		3	4.5	0.032	0.020	0.007	0.000	-0.002	0.004	0.015	-0.003	0.0017	0.0053				
		4	6.0	0.032	0.017	0.006	-0.001	-0.002	0.005	0.019	-0.003	0.0023	0.0059				
		5	7.5	0.021	0.011	0.001	-0.004	-0.003	0.005	0.019	-0.002	0.0026	0.0054				
		6	9.0	0.012	0.004	-0.005	-0.009	-0.006	0.003	0.020	-0.002	0.0032	0.0056				
		7	10.5	0.002	-0.004	-0.011	-0.011	-0.011	0.000	0.016	-0.001	0.0031	0.0046				
		AVERAGE	0.023	0.012	0.001	-0.005	-0.005	-0.005	0.002	0.014	-0.003	0.0021	0.0053				
1-5	15" X 18" X 3/8"	1	1.5	0.009	0.005	0.008	0.010	0.007	0.014	0.000	0.002	-0.0000	-0.0010	0.000	0.000	0.000	0.000
		2	3.0	0.012	0.007	0.012	0.012	0.009	0.017	0.001	0.002	-0.0000	-0.0010				
		3	4.5	0.015	0.010	0.013	0.015	0.011	0.019	0.002	0.001	-0.0010	-0.0011				
		4	6.0	0.016	0.010	0.014	0.016	0.012	0.022	0.003	0.001	-0.0010	-0.0011				
		5	7.5	0.023	0.016	0.029	0.020	0.013	0.024	0.004	0.001	-0.0012	-0.0014				
		6	9.0	0.024	0.011	0.015	0.010	0.014	0.022	0.005	0.001	-0.0010	-0.0010				
		7	10.5	0.024	0.011	0.016	0.017	0.014	0.022	0.007	0.001	-0.0010	-0.0010				
		8	12.0	0.024	0.010	0.014	0.015	0.012	0.020	0.003	0.001	-0.0010	-0.0010				
		9	13.5	0.025	0.010	0.012	0.013	0.010	0.019	0.003	0.001	-0.0010	-0.0010				
		AVERAGE	0.019	0.010	0.015	0.015	0.011	0.011	0.020	0.003	0.002	-0.0009	-0.0007				
1-6	18" X 18" X 3/8"	1	1.5	-0.010	-0.007	-0.000	-0.010	-0.010	-0.000	0.000	0.000	0.0011	0.0011	0.000	0.000	0.000	0.000
		2	3.0	-0.012	-0.010	-0.011	-0.011	-0.011	-0.010	-0.000	0.001	0.0003	0.0003				
		3	4.5	-0.012	-0.010	-0.012	-0.012	-0.015	-0.010	-0.004	0.001	0.0010	0.0010				
		4	6.0	-0.008	-0.006	-0.009	-0.011	-0.011	-0.000	-0.006	0.000	0.0006	0.0010				
		5	7.5	-0.010	-0.008	-0.012	-0.013	-0.015	-0.011	-0.010	0.000	0.0004	0.0009				
		6	9.0	-0.011	-0.009	-0.013	-0.014	-0.016	-0.011	-0.000	0.000	0.0006	0.0012				
		7	10.5	-0.010	-0.010	-0.012	-0.014	-0.016	-0.011	-0.005	0.001	0.0005	0.0015				
		8	12.0	-0.011	-0.010	-0.014	-0.011	-0.015	-0.011	-0.007	0.001	0.0005	0.0007				
		9	13.5	-0.011	-0.010	-0.012	-0.015	-0.010	-0.011	-0.008	0.001	0.0005	0.0014				
		10	15.0	-0.012	-0.010	-0.012	-0.012	-0.016	-0.011	-0.008	0.001	0.0006	0.0006				
		11	16.5	-0.011	-0.011	-0.013	-0.014	-0.017	-0.011	-0.000	0.000	0.0000	0.0012				
		AVERAGE	-0.011	-0.009	-0.012	-0.012	-0.012	-0.015	-0.010	-0.007	0.003	0.0007	0.0010				

TABLE 4.4 PRE-HEATING DATA AND CALCULATED ANGULAR DEFLECTIONS - FOLLOW-ON EXPERIMENT # 1

PLATE #	DIMENSIONS	GRID LINE #	OUT OF PLANE DISTORTION							ANGULAR DEFLECTION			
			X	Y	6.0	9.0	12.0	15.0	10.0	A1f	A2f	Grad-	THETAf
1-1	3" X 10" X 3/8"	1	1.5	-0.035	-0.032	-0.030	-0.035	-0.025	0.000	0.0001	0.0030	0.0030	0.0030
		AVERAGE		-0.035	-0.032	-0.030	-0.035	-0.025	0.000	0.0001	0.0030	0.0030	0.0030
1-2	6" X 10" X 3/8"	1	1.5	-0.235	-0.250	-0.254	-0.242	-0.172	0.000	-0.0000	0.0271	0.0271	0.0200
		2	3.0	-0.233	-0.240	-0.252	-0.244	-0.174	-0.011	-0.0012	0.0262	0.0262	0.0274
		3	4.5	-0.232	-0.250	-0.256	-0.247	-0.181	-0.026	-0.0017	0.0240	0.0240	0.0265
		AVERAGE		-0.233	-0.249	-0.254	-0.244	-0.176	-0.012	-0.0013	0.0261	0.0261	0.0273
1-3	9" X 10" X 3/8"	1	1.5	-0.140	-0.132	-0.137	-0.130	-0.106	0.000	0.0000	0.0154	0.0154	0.0154
		2	3.0	-0.132	-0.129	-0.135	-0.136	-0.102	0.000	-0.0006	0.0160	0.0160	0.0166
		4	6.0	-0.130	-0.126	-0.135	-0.135	-0.100	0.013	-0.0007	0.0165	0.0165	0.0173
		5	7.5	-0.133	-0.131	-0.139	-0.141	-0.104	0.016	-0.0011	0.0175	0.0175	0.0186
		AVERAGE		-0.133	-0.129	-0.136	-0.137	-0.102	0.011	-0.0006	0.0165	0.0165	0.0171
1-4	12" X 10" X 3/8"	1	1.5	-0.030	-0.040	-0.064	-0.074	-0.056	0.000	-0.0049	0.0002	0.0002	0.0131
		2	3.0	-0.026	-0.045	-0.060	-0.069	-0.050	0.005	-0.0040	0.0003	0.0003	0.0131
		3	4.5	-0.026	-0.045	-0.059	-0.067	-0.047	0.015	-0.0046	0.0001	0.0001	0.0137
		4	6.0	-0.032	-0.046	-0.060	-0.066	-0.046	0.019	-0.0039	0.0004	0.0004	0.0133
		5	7.5	-0.030	-0.049	-0.061	-0.069	-0.047	0.017	-0.0035	0.0009	0.0009	0.0134
		6	9.0	-0.047	-0.055	-0.060	-0.073	-0.040	0.020	-0.0030	0.0103	0.0103	0.0133
		7	10.5	-0.055	-0.065	-0.073	-0.076	-0.050	0.020	-0.0024	0.0106	0.0106	0.0130
1-5	15" X 10" X 3/8"	AVERAGE		-0.036	-0.050	-0.064	-0.071	-0.049	0.014	-0.0039	0.0094	0.0094	0.0133
		1	1.5	0.006	0.056	0.034	0.012	0.007	0.000	-0.0001	-0.0009	0.0072	0.0072
		2	3.0	0.000	0.057	0.036	0.013	0.000	0.000	-0.0002	-0.0010	0.0072	0.0072
		3	4.5	0.000	0.050	0.036	0.014	0.000	0.000	-0.0003	-0.0011	0.0072	0.0072
		4	6.0	0.000	0.059	0.036	0.013	0.009	0.001	-0.0005	-0.0009	0.0075	0.0075
		5	7.5	0.000	0.050	0.036	0.012	0.010	0.001	-0.0005	-0.0009	0.0077	0.0077
		6	9.0	0.000	0.059	0.035	0.011	0.009	0.000	-0.0007	-0.0008	0.0079	0.0079
		7	10.5	0.009	0.050	0.032	0.011	0.009	0.000	-0.0007	-0.0009	0.0070	0.0070
		8	12.0	0.009	0.050	0.032	0.009	0.009	0.001	-0.0009	-0.0006	0.0083	0.0083
		9	13.5	0.093	0.053	0.031	0.000	0.006	0.000	-0.0092	-0.0005	0.0087	0.0087
1-6	10" X 16" X 3/8"	AVERAGE		0.009	0.057	0.034	0.011	0.000	0.000	-0.0006	-0.0009	0.0077	0.0077
		1	1.5	0.119	0.091	0.052	0.010	0.011	0.000	-0.0122	-0.0011	0.0111	0.0111
		2	3.0	0.110	0.090	0.051	0.010	0.009	-0.007	-0.0113	-0.0027	0.0086	0.0086
		3	4.5	0.110	0.091	0.050	0.010	0.007	-0.005	-0.0114	-0.0023	0.0090	0.0090
		4	6.0	0.124	0.096	0.054	0.010	0.001	-0.006	-0.0120	-0.0022	0.0090	0.0090
		5	7.5	0.125	0.095	0.051	0.015	0.000	-0.004	-0.0125	-0.0021	0.0104	0.0104
		6	9.0	0.125	0.095	0.052	0.017	0.000	-0.002	-0.0122	-0.0020	0.0102	0.0102
		7	10.5	0.124	0.094	0.052	0.010	0.007	0.000	-0.0120	-0.0010	0.0102	0.0102
		8	12.0	0.125	0.094	0.054	0.010	0.000	-0.002	-0.0120	-0.0021	0.0099	0.0099
		9	13.5	0.126	0.094	0.054	0.016	0.000	-0.004	-0.0123	-0.0021	0.0102	0.0102
		10	15.0	0.126	0.094	0.053	0.010	0.000	-0.003	-0.0122	-0.0022	0.0100	0.0100
		11	16.5	0.127	0.091	0.052	0.019	0.007	-0.002	-0.0121	-0.0021	0.0100	0.0100
AVERAGE				0.123	0.093	0.052	0.017	0.007	-0.003	-0.0120	-0.0021	0.0099	0.0099

TABLE 4.5 POST-HEATING DATA AND CALCULATED ANGULAR DEFLECTIONS - FOLLOW-ON EXPERIMENT # 1

GRID LINE #	OUT OF PLANE DISTORTION					Y	ANGULAR DEFLECTION							
	X	0.00	1.50	4.50	7.50		10.50	13.50	16.50	10.00	THETA	CHANGE		
0 7 6 5 4 3 2 1	0	0.75	0.170	0.152	0.086	0.013	INITIAL PLATE					-0.003	0.0240	0.0000
	7	2.25	0.173	0.140	0.083	0.014	-0.023	-0.012	-0.005	-0.011	0.0236	0.0000		
	6	3.75	0.173	0.140	0.085	0.010	-0.027	-0.010	-0.012	-0.011	0.0233	0.0000		
	5	5.25	0.172	0.149	0.080	0.009	-0.030	-0.027	-0.025	-0.024	0.0229	0.0000		
	4	6.75	0.170	0.140	0.078	0.010	-0.031	-0.030	-0.020	-0.020	0.0230	0.0000		
	3	8.25	0.173	0.156	0.079	0.007	-0.032	-0.030	-0.031	-0.032	0.0228	0.0000		
	2	9.75	0.176	0.156	0.081	0.010	-0.030	-0.030	-0.031	-0.034	0.0223	0.0000		
	1	11.25	0.106	0.100	0.082	0.010	-0.029	-0.030	-0.032	-0.034	0.0233	0.0000		
0 7 6 5 4 3 2 1	0	0.75	0.100	0.156	0.008	0.017	FIRST CUT					-0.004	0.0253	0.0005
	7	2.25	0.105	0.155	0.007	0.016	-0.022	-0.012	-0.005	-0.011	0.0246	0.0011		
	6	3.75	0.105	0.155	0.005	0.015	-0.020	-0.010	-0.019	-0.015	0.0244	0.0011		
	5	5.25	0.106	0.156	0.006	0.014	-0.030	-0.026	-0.023	-0.021	0.0242	0.0014		
	4	6.75	0.109	0.156	0.008	0.009	-0.029	-0.025	-0.025	-0.023	0.0247	0.0017		
	3	8.25	0.192	0.163	0.005	0.013	-0.030	-0.027	-0.026	-0.025	0.0249	0.0020		
	2	9.75	0.190	0.165	0.090	0.012	-0.025	-0.025	-0.024	-0.024	0.0251	0.0020		
	1	11.25	0.123	0.100	0.050	-0.001	-0.034	-0.033	-0.032	-0.034	0.0167	-0.0006		
0 7 6 5 4 3 2 1	0	0.75	0.193	0.161	0.094	0.024	SECOND CUT					-0.005	0.0244	-0.0009
	7	2.25	0.191	0.160	0.091	0.010	-0.023	-0.012	-0.015	-0.012	0.0240	0.0002		
	6	3.75	0.186	0.156	0.087	0.014	-0.033	-0.025	-0.019	-0.017	0.0252	0.0007		
	5	5.25	0.180	0.157	0.080	0.011	-0.033	-0.028	-0.022	-0.021	0.0253	0.0011		
	4	6.75	0.191	0.157	0.080	0.014	-0.032	-0.020	-0.026	-0.023	0.0247	-0.0001		
	3	8.25	0.195	0.163	0.090	0.014	-0.030	-0.025	-0.023	-0.025	0.0250	0.0001		
	2	9.75	0.169	0.140	0.075	0.010	-0.024	-0.022	-0.024	-0.024	0.0212	-0.0030		
	1	11.25	0.123	0.100	0.050	-0.001	-0.034	-0.033	-0.032	-0.034	0.0167	0.0000		
0 7 6 5 4 3 2 1	0	0.75	0.222	0.107	0.116	0.040	THIRD CUT					0.000	0.0250	0.0006
	7	2.25	0.221	0.107	0.114	0.036	-0.006	-0.007	-0.005	-0.006	0.0253	0.0005		
	6	3.75	0.224	0.190	0.114	0.036	-0.011	-0.011	-0.009	-0.009	0.0255	0.0003		
	5	5.25	0.227	0.192	0.115	0.037	-0.014	-0.013	-0.012	-0.012	0.0257	0.0004		
	4	6.75	0.231	0.195	0.121	0.036	-0.012	-0.011	-0.012	-0.012	0.0259	0.0012		
	3	8.25	0.105	0.153	0.089	0.010	-0.026	-0.023	-0.025	-0.025	0.0226	-0.0033		
	2	9.75	0.169	0.140	0.075	0.010	-0.024	-0.022	-0.024	-0.024	0.0212	0.0000		
	1	11.25	0.123	0.100	0.050	-0.001	-0.034	-0.033	-0.032	-0.034	0.0167	0.0000		

TABLE 4.7 EFFECT OF SECTIONING PLATE 0-4: FIRST THROUGH THIRD CUT

GRID LINE #	OUT OF PLANE DISTORTION							ANGULAR DEFLECTION			
	X	0.00	1.50	4.50	7.50	Y	10.50	13.50	16.50	18.00	THETAT CHANGE
FOURTH CUT											
0	0.75	0.232	0.190	0.122	0.044	-0.003	-0.002	-0.002	-0.002	-0.002	0.0253 0.0002
7	2.25	0.234	0.190	0.126	0.044	-0.005	-0.002	-0.003	-0.002	-0.005	0.0253 0.0001
6	3.75	0.241	0.201	0.128	0.047	-0.003	-0.003	-0.003	-0.003	-0.005	0.0255 -0.0000
5	5.25	0.250	0.210	0.135	0.052	-0.002	-0.001	-0.001	-0.003	-0.002	0.0262 0.0004
4	6.75	0.260	0.164	0.087	0.015	-0.020	-0.024	-0.024	-0.024	-0.025	0.0242 -0.0017
3	8.25	0.165	0.153	0.069	0.015	-0.026	-0.023	-0.023	-0.025	-0.025	0.0226 0.0000
2	9.75	0.169	0.140	0.075	0.010	-0.024	-0.024	-0.022	-0.024	-0.024	0.0212 0.0000
1	11.25	0.123	0.100	0.050	-0.001	-0.034	-0.034	-0.033	-0.032	-0.034	0.0167 0.0000
FIFTH CUT											
0	0.75	0.247	0.211	0.137	0.057	0.005	0.004	0.004	0.001	-0.002	0.0244 -0.0009
7	2.25	0.250	0.214	0.135	0.056	0.001	0.002	0.000	-0.003	-0.006	0.0240 -0.0006
6	3.75	0.253	0.219	0.137	0.054	0.002	0.000	0.000	-0.005	-0.007	0.0255 0.0000
5	5.25	0.239	0.202	0.127	0.044	-0.001	-0.002	-0.002	-0.002	-0.002	0.0250 -0.0003
4	6.75	0.200	0.164	0.087	0.015	-0.020	-0.024	-0.024	-0.024	-0.025	0.0242 0.0000
3	8.25	0.105	0.153	0.069	0.015	-0.026	-0.023	-0.023	-0.025	-0.025	0.0226 0.0000
2	9.75	0.169	0.140	0.075	0.010	-0.024	-0.022	-0.022	-0.024	-0.024	0.0212 0.0000
1	11.25	0.123	0.100	0.050	-0.001	-0.034	-0.033	-0.033	-0.032	-0.034	0.0167 0.0000
SIXTH CUT											
0	0.75	0.235	0.200	0.131	0.052	0.003	0.005	0.005	0.004	0.003	0.0243 -0.0001
7	2.25	0.240	0.205	0.129	0.054	0.004	0.005	0.005	0.003	0.002	0.0246 -0.0001
6	3.75	0.244	0.200	0.135	0.047	-0.005	-0.005	-0.005	-0.005	-0.007	0.0259 0.0004
5	5.25	0.239	0.202	0.127	0.044	-0.001	-0.002	-0.002	-0.002	-0.002	0.0250 0.0000
4	6.75	0.200	0.164	0.087	0.015	-0.020	-0.024	-0.024	-0.024	-0.025	0.0242 0.0000
3	8.25	0.105	0.153	0.069	0.015	-0.026	-0.023	-0.023	-0.025	-0.025	0.0226 0.0000
2	9.75	0.169	0.140	0.075	0.010	-0.024	-0.022	-0.022	-0.024	-0.024	0.0212 0.0000
1	11.25	0.123	0.100	0.050	-0.001	-0.034	-0.033	-0.033	-0.032	-0.034	0.0167 0.0000
SEVENTH CUT											
0	0.75	0.246	0.213	0.140	0.065	0.012	0.011	0.011	0.007	0.003	0.0231 -0.0012
7	2.25	0.250	0.210	0.140	0.056	0.003	0.004	0.004	0.002	0.002	0.0254 0.0000
6	3.75	0.244	0.200	0.135	0.047	-0.005	-0.005	-0.005	-0.005	-0.007	0.0259 0.0000
5	5.25	0.239	0.202	0.127	0.044	-0.001	-0.002	-0.002	-0.002	-0.002	0.0250 0.0000
4	6.75	0.200	0.164	0.087	0.015	-0.020	-0.024	-0.024	-0.024	-0.025	0.0242 0.0000
3	8.25	0.105	0.153	0.069	0.015	-0.026	-0.023	-0.023	-0.025	-0.025	0.0226 0.0000
2	9.75	0.169	0.140	0.075	0.010	-0.024	-0.022	-0.022	-0.024	-0.024	0.0212 0.0000
1	11.25	0.123	0.100	0.050	-0.001	-0.034	-0.033	-0.033	-0.032	-0.034	0.0167 0.0000

TABLE 4.0 EFFECT OF SECTIONING PLATE 0-1: FOURTH THROUGH SEVENTH CUT

CHAPTER 5

ANALYSIS

5.1 General

The analysis of the results presented in the previous chapter was divided into two parts: angular deflection vs. plate length and angular deflection vs. in plate location (or edge effects). The approach taken when considering bending vs. plate length was first to compare the results with the already existing body of data and secondly, to appropriate analytic models. A parametric study was performed, and parameter values related to already established parameters describing plate bending. The analysis of the edge behavior, for which less existing data is available, was less quantitative. The observed bending behavior was described in terms of a qualitative model, and an attempt to determine the relative contribution of the two principal factors made.

5.2 Angular Deflection vs. Plate Length

The analysis of the experimental data relating to this behavior considered first the validity of the results, both in the light of previous experimental data, and also with established models for thermo-mechanical bending of plates. The major source of existing experimental data used for comparison was the Phase I Report. In particular, the results of the parametric study of P/\sqrt{V} vs. θ_t . The angular deflections of the larger plates (1-6 and 2-6) corresponding to the estimated values of P/\sqrt{V} used in the two follow-on experiments were superimposed on the existing graph of P/\sqrt{V} vs. θ_t . Figure 5.1 illustrates that these added data points fall in a region between the curves depicting the behavior of the 1/4" and 1/2" plates, exhibiting the same general pattern. Additionally, the trend of increasing angular deflection at a decreasing rate noted in the preliminary and follow-on experiment, is very similar to that observed for the line heated 12"x12"x1/2" plate ($P/\sqrt{V}=1.8$) depicted in Figure 2.4, in which heating was along lines parallel to the plate edge. The laser line heating data also exhibited a similar trend. The major factor expected to influence this behavior, as discussed in Chapter 2, is related to the proximity of the plate edge. Decreasing the plate dimension in the direction of heating reduces the amount of plate

material available to provide mechanical restraint and act as a heat sink. So as plate length is reduced, the "edge effects" should progressively dominate, reducing the amount of bending in the same manner as outlined in the discussion of the expected of reducing the plate width given in Chapter 2. The transition should be a gradual one.

In this case, the angular deflection observed in a plate of a given length could possibly be determined based on the distance from the plate center to the perpendicular edge, i.e. by $L/2$. To examine this possibility, the results of the line heated $1/2$ " plates (obtained under experimental conditions that best approximated those specified in Figure 2.4), were plotted as a function of $L/2$. The curve so obtained was then superimposed on Figure 2.4. The result, depicted in Figure 5.2, is that the 2 curves essentially coincide. The implications of this correspondence is that the effect of varying the plate dimensions on bending is the same for the length as for the width, and can be predicted using the same curve that describes the bending as the line of heating approaches a plate edge parallel to it. Therefore, not only do the results appear to be in general agreement with previous experimental data, but they also afford a means of accounting for the plate dimensions in the plate bending predictions, provided the curve is known for

that particular plate and value of P/\sqrt{V} . The parametric studies discussed later in this section address how this curve should relate to P/\sqrt{V} .

The heat deformation model was used to examine quantitatively the expected large plate deflection with respect to measured top and bottom plate temperatures. The results of these calculations are summarized and compared to the experimental results in Table 5.1. The model underestimates the experimental values by a factor of approximately 2.5. This was in fact predicted by Luebke, based on results obtained during the course of his investigation. When this model was applied in his studies of bending with variations in plate thickness, it was noted that the model underestimated the distortion for plates of thickness less than approximately 0.58" and overestimated the distortion for plates of greater thickness, with the variation being a linear function of thickness over the range studied. For a plate thickness of 3/8" a correction factor of 3.0 was determined. Therefore, the corrected prediction and experimental results appear in reasonable agreement.

In order to value narrow plate deflection, the analytic model developed by Iwamura and Rybicki was considered. As mentioned in Chapter 2, a serious attempt to develop a

computer program based on the model was undertaken. However, stability problems relating to the calculation of the mechanical strain at points along lines through the plate strip could not be adequately resolved. The integration of the stress estimating functions along the thickness of the plate appeared to produce alternating stable configurations primarily during the transition from heat up to cool down. This resulted in premature termination of the iterative procedure prior to the cool down phase. Results produced during the heat up phase of the computer simulation did appear to be in agreement with observed behavior for that point of the thermal cycle, specifically that of out-of-plane distortion and angular deflection. However, the inability to carry the calculations on through the cool down phase, did not permit useful quantitative output predicting the final distribution of residual stresses and resulting deflections to be obtained. A quantitative comparison with Iwamura and Rybicki's published results is not valid due to the inherent differences in the narrow plate modeled (5mm wide, 50mm thick, 500mm long) and the experimental procedures (differences in the application of heat, use of forced cooling) as compared to those presented here. In a qualitative sense, the angular deflections (both theoretical

and experimental) that they obtained, of 3.5 milli-radians does compare favorable with those obtained for the narrow plates (plates 0-1, 12.7 milli-rads; plate 1-1, 4.5 milli-rads; plate 2-1, 7.9 milli-rads).

Characterization of the behavior, in the form of a parametric study, was then undertaken. The behavior suggested a functional relationship of the form:

$$\theta_t(L) = A(1 - e^{-BL})$$

where θ_t = total angular deflection,

L = the plate length.

Further, it was expected that both parameters, A and B, should be related to the value of P/\sqrt{V} corresponding to the experiment. Clearly, the limiting value of the relationship, A, would be the bending obtained in large plates for a given thickness, and so dependent on P/\sqrt{V} as expressed in the parametric studies of the Phase I Report. The decay constant, B, on the other hand could exhibit more dependence on velocity than provided by the parameter P/\sqrt{V} .

The results of the parametric study are contained in the Appendix. The study included the preliminary experiment, the 2 follow-on experiments, as well as the laser line heating data. It was found to be more meaningful to average the data when possible, to reduce random effects. In particular, the data of the preliminary and second follow-on

experiments were averaged for the first four plates and the laser line heating data was averaged for each of the 3 thickness of the plate considered. A summary of the parameter values, A and B, obtained in each case is given in Table 5.2, accompanied by the corresponding power and speed data. A preliminary comparison indicates that A does indeed depend on P/\sqrt{V} as previously described, and that B appears to be proportional to P/v^n , with n in the range of 0.5 to 1.5. Given the correspondence of deflective behavior with respect to distance from both the parallel and perpendicular edges, these parametric curves would then serve to predict bending of a plate based on its dimensions and the location of the line of heating.

5.3 Angular Deflection vs. In Plate Location--

Edge Effects

Given the significance of edge effects on the bending of narrow plates, a more detailed study of these effects was conducted. Commencing with the preliminary experiment, the 0-4 plate was cut as previously described to provide information that could serve as a basis for such a study. The most immediate result was that of the asymmetry in the behavior. Differing from the previously discussed symmetric behavior as heating along lines parallel to the plate edge

progresses from one edge to the other (neglecting any differing residual stress distributions already present), the plate exhibits varying amounts of bending as the heat source enters over and exits the corresponding perpendicular (to the line of heating) edges. This variation was noted in the majority of the plates studied, generally presenting the same pattern. This pattern was of reduced bending at the entrance edge of the heating source, increasing at an increasing rate over a portion of the interior, then at essentially constant rate, until approaching the far edge of the plate where bending again decreased but not as much as at the entrance. The angular deflection profile, graphed in Figure 5.3, of the cut plate segments clearly illustrates this asymmetry. A quadratic least squares fit resulted in a very close correspondence. The plate strips had been cut out sequentially, progressing in the same direction as the heat source, with the first strip cut being centered about the 11.25" grid line. The bending at this edge was approximately 75% of that at the far edge and 64% of the maximum bending as measured in the free strips.

An attempt to verify similar behavior in other plates, without the need to section each plate, led to performing the linear and quadratic least squares curve fittings to the data corresponding to the first follow-on experiment (plates

1-3 through 1-6; plates 1-1 and 1-2 were purposely excluded as being too narrow) mentioned in Chapter 4. The graphs, given in Figures 5.4 through 5.7, show the same behavior in 2 of the 4 plates. In all cases, the general trend is for angular deflection to increase through the length of the plate interior. The marked differences in the other two plates (1-4 and 1-6) are expected to be principally due to unrelieved stresses from the plate forming process, i.e. rolling, press cut, etc. A qualitative description of the expected mechanism producing this behavior is outlined in the following paragraph.

Consider that an effective length exists, which defines the plate material adjacent to that being heated by the torch, that contributes directly to the restraint experienced by the material under the torch. Further, that the plate is divided into strips perpendicular to the direction of travel, of width given by this effective length. As the heat source moves over the first such strip, the bending that will be produced is determined by the restraint provided by the adjacent interior strip and the thermal gradient through the plate. Neglecting the thermal gradient effect, this strip sees "one unit" of restraint as it begins to deflect downward. As the heat source moves over the second strip, the out board strip is starting to approach

zero deflection so this second strip is subject to essentially "2 units" of restraint (one from each adjacent strip). The third strip will likewise receive "2 units" of restraint from the second and fourth strips, but the first is now deflecting positively and will, through the second strip, provide an additional restraining moment. The third strip is then subjected to "3 units" of restraint. The sequence will repeat itself, with the restraint increasing for each successive strip, as previously heated strips cool and continue to deflect positively. Sufficiently into the plate interior, the first strips will have attained maximum positive deflection and so no longer act to increase the restraining moment; each successive strip is receiving the same amount of restraint. Finally, as the far edge is approached, the available restraint decreases. The amount of bending produced in each strip, varies in a likewise manner.

The reduced temperature gradient at the edges, neglected in the above, also influences the bending. This then leads to the question of the relative contribution of each effect; reduced material restraint and reduced temperature difference between the top and bottom surfaces of the plate. An attempt to provide an answer was made using the heat deformation model to estimate the thermal contribution,

and then comparing this with the total effect as seen in the cut plate. The representative temperature measurements taken at the near edge and interior, at both top and bottom surfaces were used to calculate the bending that would be expected due to temperature effects only. The results of the calculations, including intermediate values used in the heat deformation model, have been already given in Table 5.1. The ratio of the angular deflections corresponding to the temperatures at the edge to that of the temperatures of the plate interior was found to be 0.91. The ratios of the edge deflections to the maximum deflection for the cut plate were found to be 0.65 for the entrance edge and 0.92 for the exiting edge. This would indicate that the major effect at the entrance edge is that of the decreased material restraint, accounting for approximately 70% of the reduction in bending at that edge. At the exiting edge, the situation appears more complicated. The mechanical restraint due to the deforming geometry of the plate interior would appear to act in opposition to the combined effect, resulting in the 0.92 ratio. A similar calculation was performed for the temperatures recorded for the first follow-on experiment, with values also given in Table 5.1. However, comparisons with the recorded data for that experiment proved less

conclusive, with most plates showing ratios of edge deflection to interior deflection of approximately 0.95.

The inconclusive nature of these last comparisons could be interpreted as an indication that other related secondary factors, such as that of geometric restraint, are also contributing to the behavior, particularly at the exiting edge. Since the variations in bending being considered are relatively small and close to the limits of the measurement techniques used, further experiments focusing on this aspect should be performed. The increased data would reduce the random influence of pre-stress conditions of the plate. If the coefficients describing the quadratic behavior can be determined for a plate then this would provide a means of predicting the actual bending produced at any point on the plate surface.

LOCATION		TEMPERATURES (deg C)		INTERMEDIATE MODEL VARIABLES			ANGULAR DEFLECTIONS (rads)	
PLATE (TO EDGE)		TOP	BOTTOM	Th	Tr	n	w	MODEL CORRECTED ACTUAL
1-6	0.5"	500.6	221.3	406.9	221.3	0.225"	0.775"	0.0042 0.0125 0.0090
P/V=1.5	5.0"	500.6	209.0	414.1	209.0	0.225"	0.695"	0.0044 0.0131 0.0090
2-6	0.5"	1000.0	506.2	705.0	506.2	0.278"	1.149"	0.0124 0.0373 0.0399
P/V=2.5	5.0"	1000.0	461.7	757.0	461.7	0.274"	1.176"	0.0136 0.0400 0.0399

TABLE 5.1 HEAT DEFORMATION MODEL PREDICTED DEFLECTIONS COMPARED TO EXPERIMENTAL RESULTS

EXPERIMENT	PLATE THICKNESS	THERMAL POWER (in/wm)	SPEED	PARAMETER A	VALUES B	ERROR **	THETAT# (rads)	P/V^n (n=0.5)	P/V^n (n=1.5)
PRELIMINARY	3/8"	6.800	7.500	43.900	0.078	18.690	- . -	2.483	0.331
FOLLOW-ON # 1	3/8"	4.100	7.500	9.500	0.280	5.120	- . -	1.497	0.200
FOLLOW-ON # 2	3/8"	6.800	7.500	55.000	0.074	183.160	- . -	2.483	0.331
PRE AND FOL-ON # 2	3/8"	6.800	7.500	51.700	0.075	20.860	- . -	2.483	0.331
LASER # 1	3/8"	6.000	9.000	10.000	0.076	20.800	- . -	2.000	0.222
LASER # 2	3/8"	6.000	5.800	24.300	0.082	5.940	- . -	2.491	0.430
LASER # 1 AND # 2	3/8"	6.000	7.400	14.600	0.110	5.877	- . -	2.206	0.290
LASER # 3	1/2"	5.000	7.700	45.200	0.062	74.560	0.019	1.802	0.234
LASER # 4	1/2"	5.000	4.000	29.800	0.320	28.640	0.026	2.500	0.625
LASER # 3 AND # 4	1/2"	5.000	5.900	35.000	0.110	1.143	0.023	2.058	0.349
LASER # 5	5/8"	8.000	7.100	30.700	0.103	3.460	0.014	3.002	0.423
LASER # 6	5/8"	8.000	5.200	32.300	0.157	2.070	0.019	3.500	0.675
LASER # 5 AND # 6	5/8"	8.000	6.200	36.030	0.121	2.800	0.017	3.213	0.518

NOTES: * ESTIMATED VALUES FROM EXISTING P/V^n vs THETAT CURVES
 ** SUM OF THE SQUARES OF THE DIFFERENCE OF THE DATA AND THE CURVE

TABLE 5.2 RESULTS OF PARAMETRIC STUDY

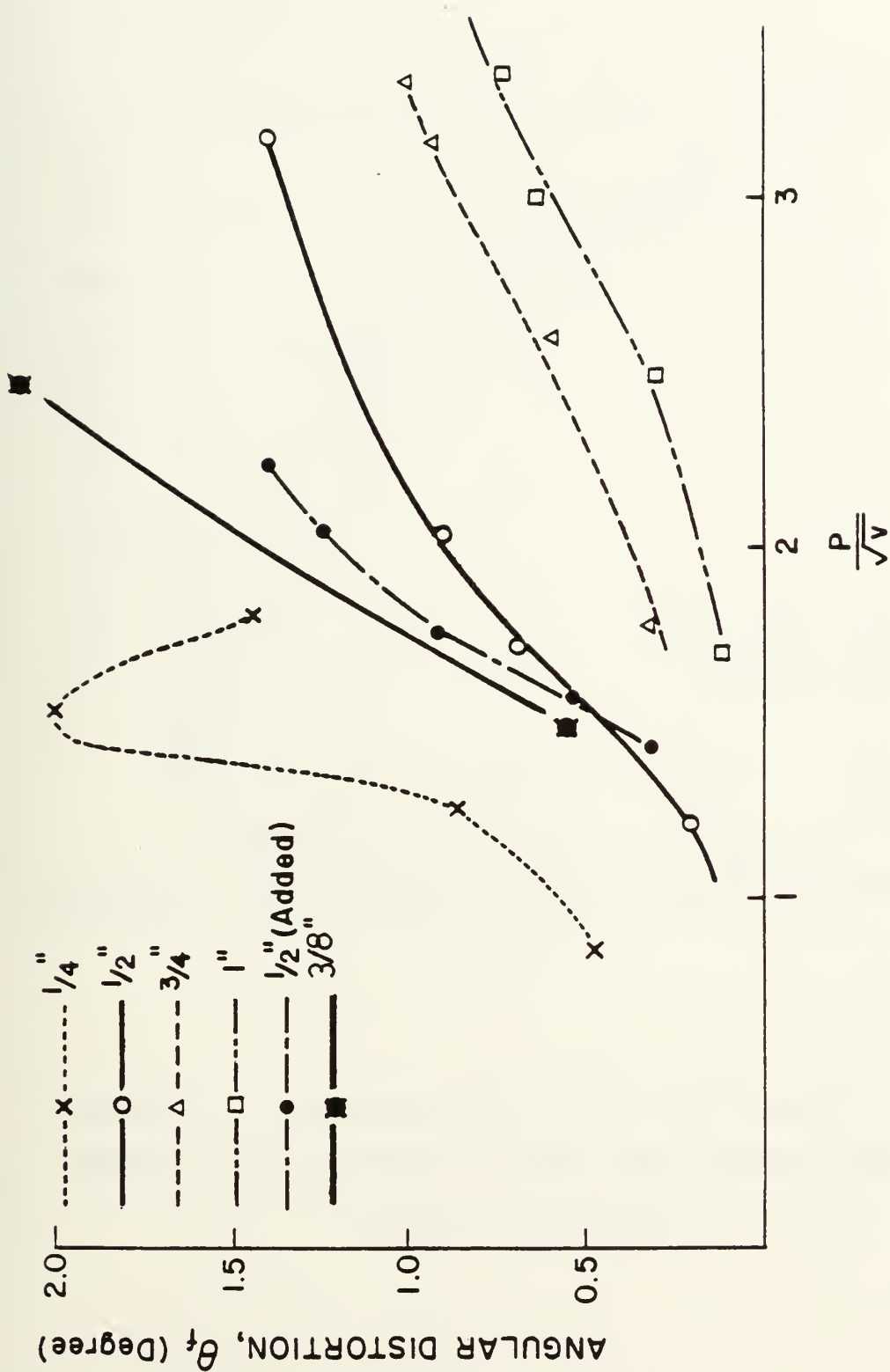
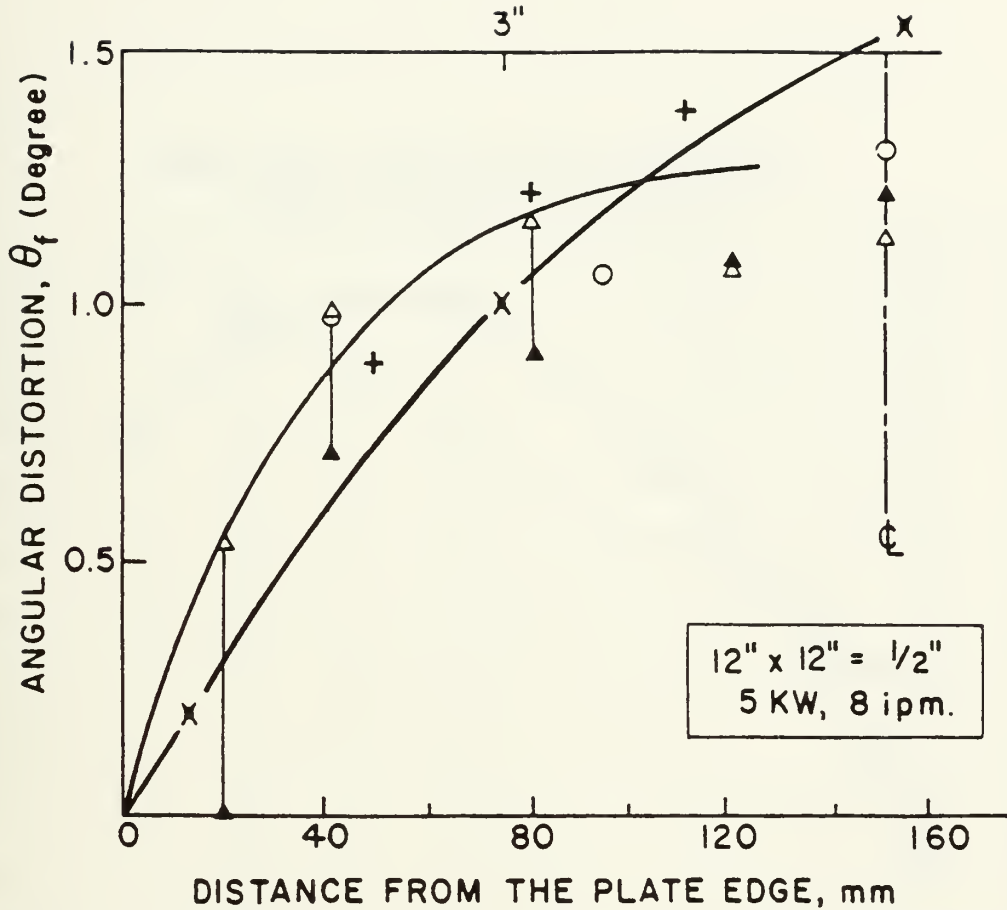


FIGURE 5.1 ADDITION OF 3/8" PLATE FLAME HEATING DATA TO EXISTING PARAMETRIC CURVES



—X—INDICATES VALUES OF θ_f PLOTTED AT DISTANCES CORRESPONDING TO HALF THE PLATE LENGTH FOR LASER HEATED ($P/V=2.1$) 1/2" PLATE

FIGURE 5.2 COMPARISON OF THE EFFECT OF LOCATION OF HEAT SOURCE WITH THE EFFECT OF VARIATION IN PLATE LENGTH ON ANGULAR DEFLECTION

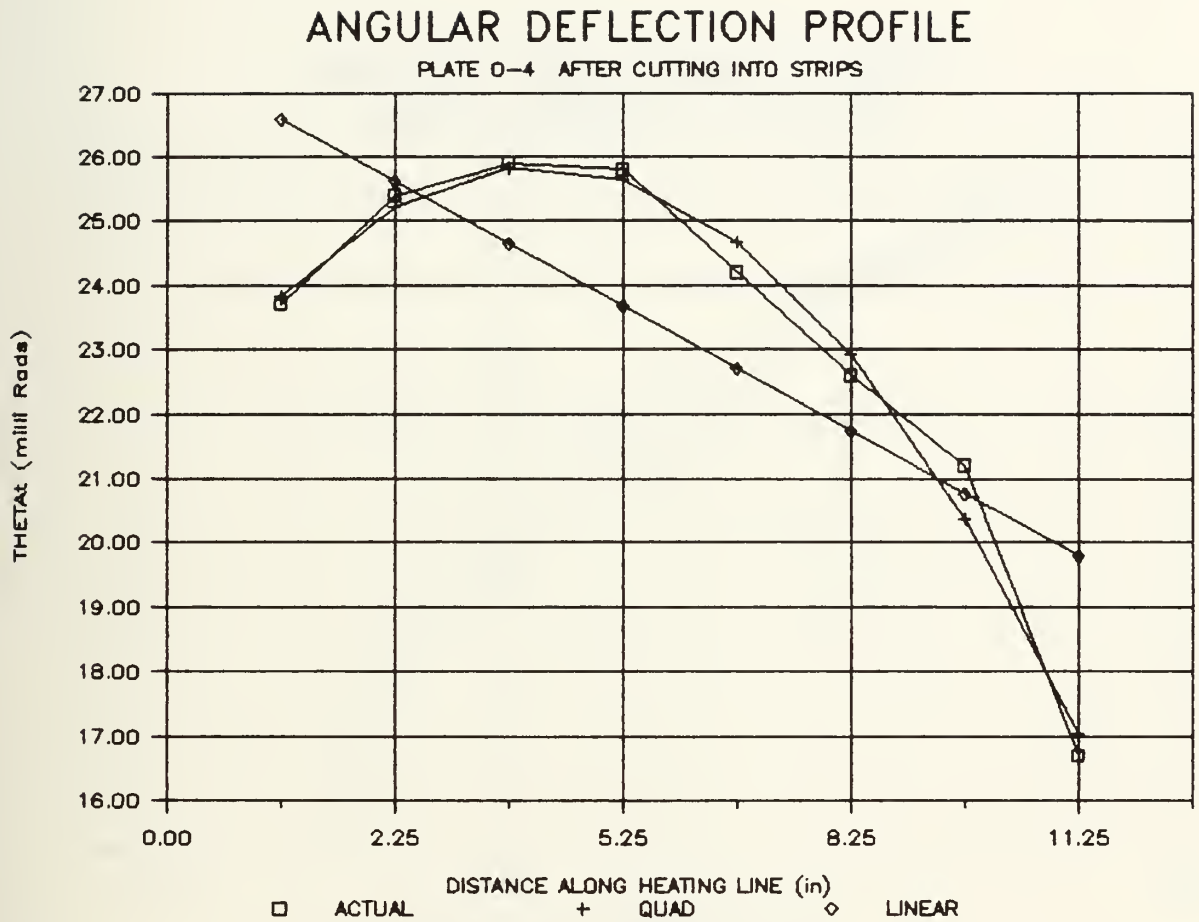


FIGURE 5.3 ANGULAR DEFLECTION PROFILE: PLATE 0-4 AFTER CUTTING

ANGULAR DEFLECTION PROFILE

PLATE 1-3 DIMENSIONS: 9" X 18" X 3/8"

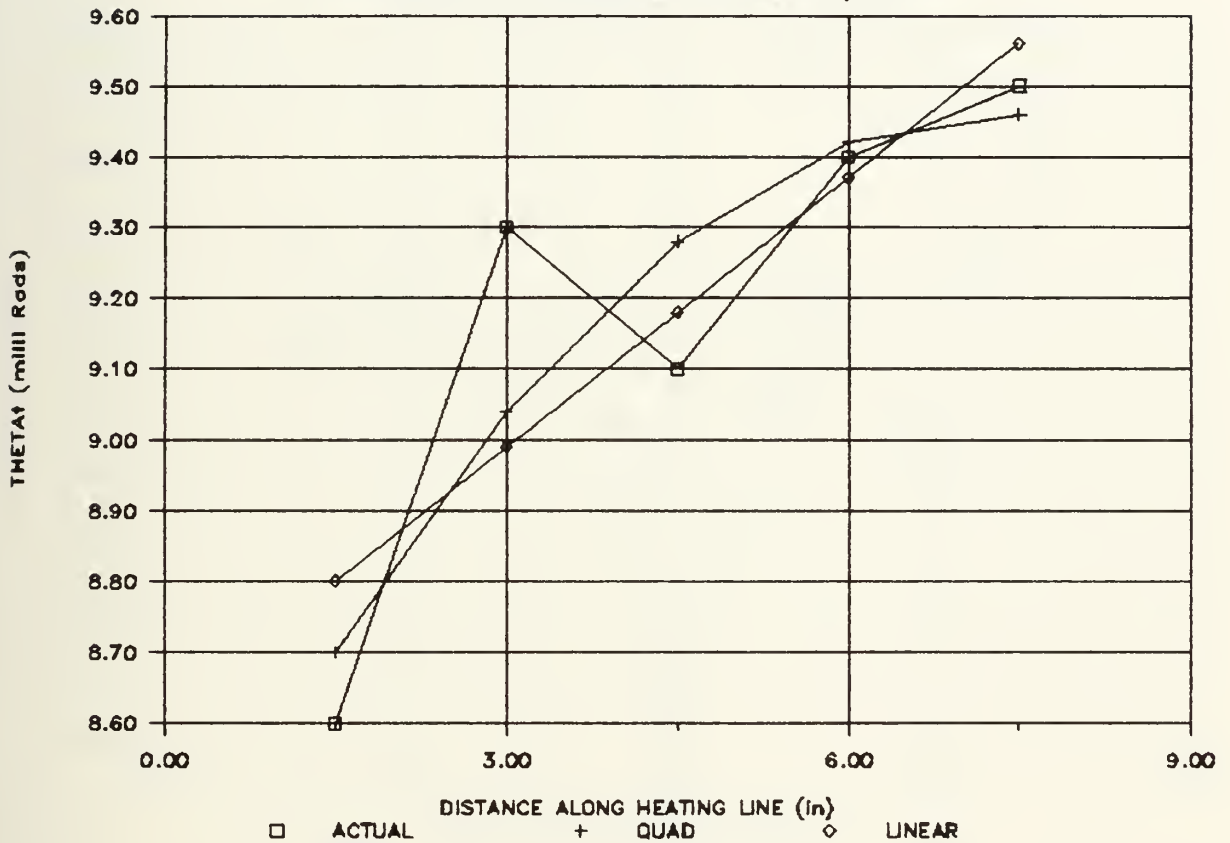


FIGURE 5.4 ANGULAR DEFLECTION PROFILE; PLATE 1-3

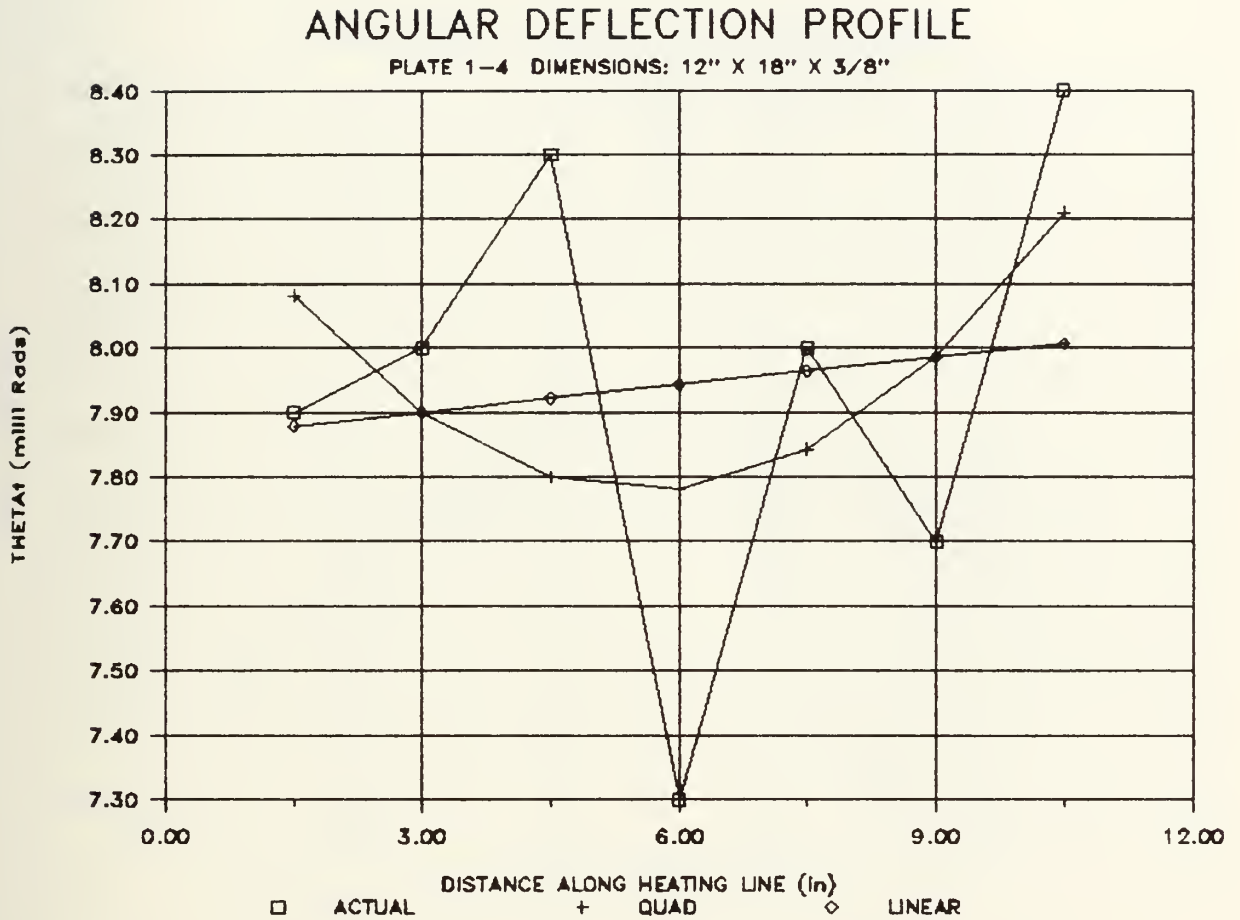


FIGURE 5.5 ANGULAR DEFLECTION PROFILE: PLATE 1-4

ANGULAR DEFLECTION PROFILE

PLATE 1-5 DIMENSIONS: 15" X 18" X 3/8"

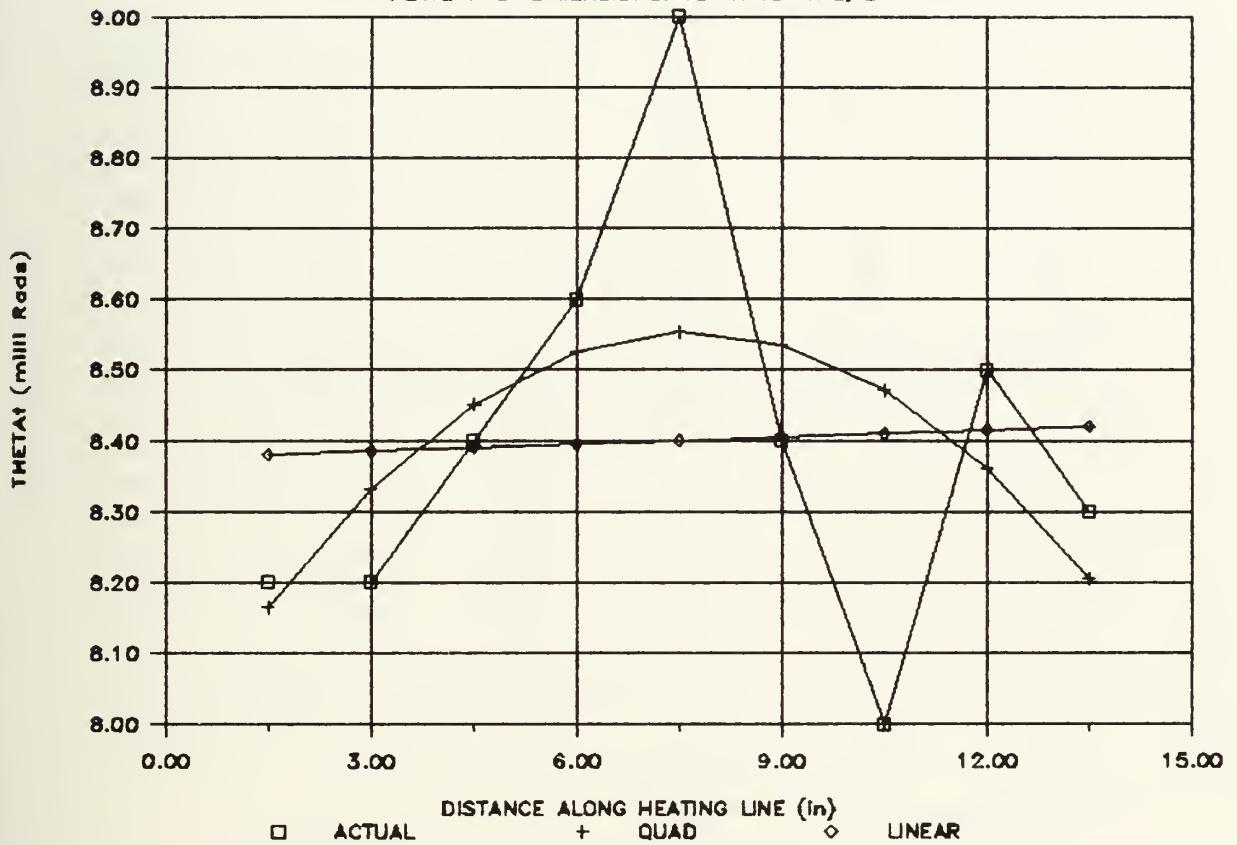


FIGURE 5.6 ANGULAR DEFLECTION PROFILE: PLATE 1-5

ANGULAR DEFLECTION PROFILE

PLATE 1-6 DIMENSIONS: 18" X 18" X 3/8"

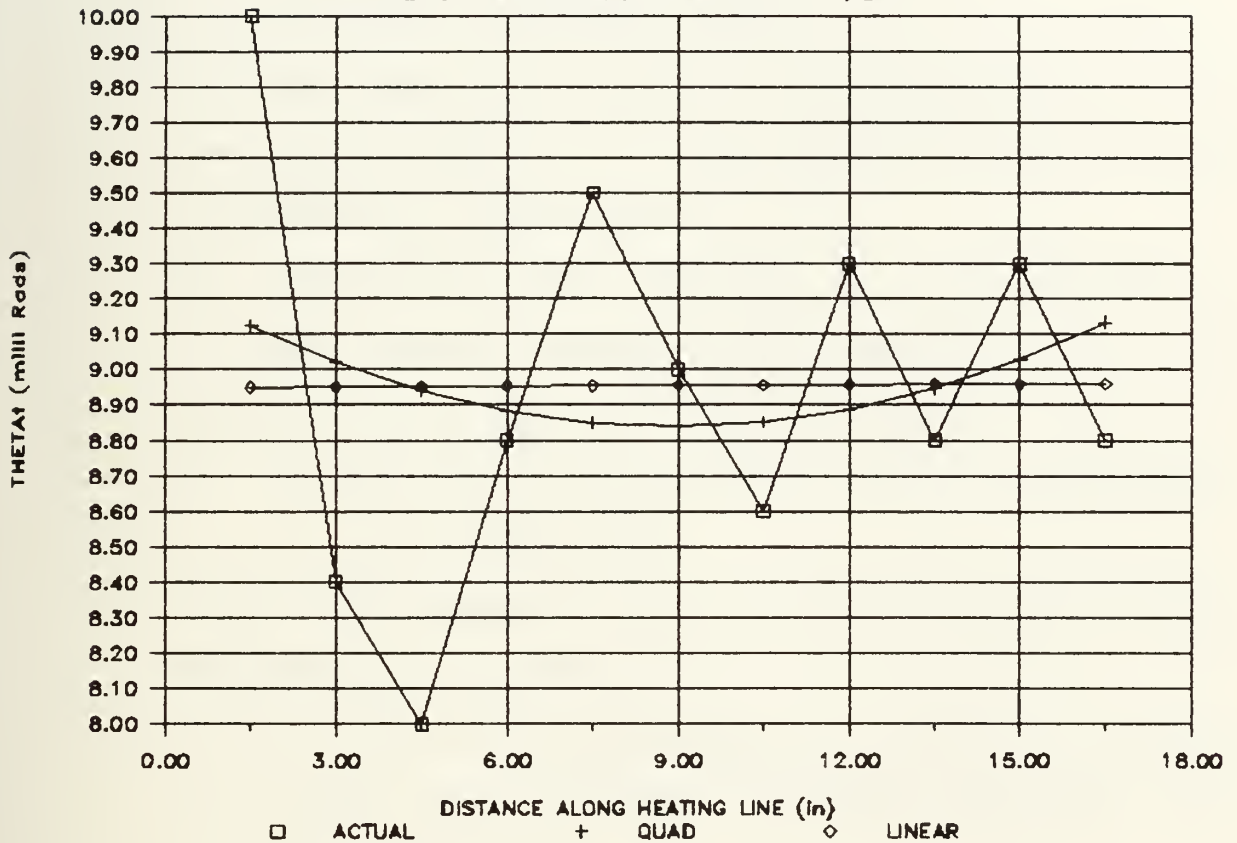


FIGURE 5.7 ANGULAR DEFLECTION PROFILE: PLATE 1-6

CHAPTER 6

CONCLUSIONS

The analysis presented leads to the following conclusions:

Angular deflection vs. plate length

1. The observed behavior of decreasing bending with decreasing length is a direct result of the increasing influence of "edge effects."
2. The average plate deflection for a given length, L , is found to be the same as that determined for heating parallel to an edge at a distance of $L/2$.
3. The behavior can be characterized by the relation:

$$\theta_t(L) = A(1 - e^{-BL}),$$

where the parameters A and B can be related to physical parameters as follows:

- i) A is directly dependent on P/\sqrt{V} in the same manner that parametric studies have shown θ_t to depend on P/\sqrt{V} .
- ii) B is proportional to P/V^n with n estimated to be in the range of 0.5 to 1.5.

Angular deflection vs. in place location

1. The observed bending behavior along the line of heating varies in a manner similar to that of when the

distance between the line of heating to a parallel edge is varied, but is not symmetrical with respect to the plate center.

2. This asymmetry is a consequence of the different orientation of the edge considered, and can be explained qualitatively from basic factors influencing bending, i.e. available material restraint.

3. This variation in bending with location appears parabolic in nature subject to the following conditions:

- i) the shape is concave down;

- ii) the bending at the entrance edge is less than that at the exiting edge of the plate with respect to heat source movement.

4. Of the two effects contributing to the bending at the edges (i.e. that of reduced material restraint and reduced temperature variation (gradient) through the plate), the reduced material restraint appears to dominate.

It should be noted that an important consequence of the above conclusions is that a model for predicting the actual bending at any point in a plate can be readily formulated.

The effects of plate length in the direction of heating and of the distance of the line of heating from a parallel edge on angular deflection can be determined as described above. Likewise, the effect of position along the line of heating on deflection could be determined using the parabolic characterization described above. The combination of these would provide the angular deflection at a given point. However, further studies of a parametric nature would be required to determine appropriate coefficients describing the parabolic behavior.

In summary, the conclusions presented above provide a better understanding of the bending behavior in plates of varying dimensions (length and width). Additionally, this behavior can be characterized in terms of parameters related to physical inputs to the thermo-mechanical forming process i.e. power and speed. Thus permitting the development of a model capable of predicting bending that can incorporate the actual dimensions of the plate, and the location and orientation of the proposed line of heating. This predictor model can be readily integrated with existing algorithms used to predict the general large plate deflection. Moreover, this model could be extended to include actual variations in bending within the plate if additional studies can verify and characterize the apparent parabolic behavior

observed. Therefore, the conclusions achieved in this study have contributed significantly to answering the questions that originally motivated the investigation.

REFERENCES

1. Masubuchi, Koichi. "Phase I Report on Laser Forming of Steel Plates for Ship Construction." Submitted to Todd Shipyards Corporation, Los Angeles Division, February 1985.
2. McCarthy, R. W. "Thermomechanical Forming of Steel Plates Using Laser Line Heat." S. M. Thesis, Department of Ocean Engineering, M.I.T., Cambridge, MA, June 1984.
3. Masubuchi, Koichi. *Analysis of Welded Structures*. Oxford: Pergamon Press, 1980.
4. Iwamura, Y., and E. F. Rybicki. "A Transient Elastic-plastic Thermal Stress Analysis of Flame Forming." *Journal of Engineering for Industry*. February, 1973: 163-171.
5. Iwasaki, Y., et al. "Study on the Forming of Hull Plate by Line Heating Method." *Technical Review*. October, 1975: 161-170.
6. Luebke, W. H., "Thermo-Mechanical Plate Forming System Concepts Using Laser Line Heating" PhD Thesis, Department of Ocean Engineering, M I T, Cambridge, MA, in preparation

REFERENCES

(Continued)

7. Boley, B. A. and J. H. Weiner, "Theory of Thermal Stresses" John Wiley & Sons, Inc., 1960

APPENDIX

PARAMETRIC STUDY

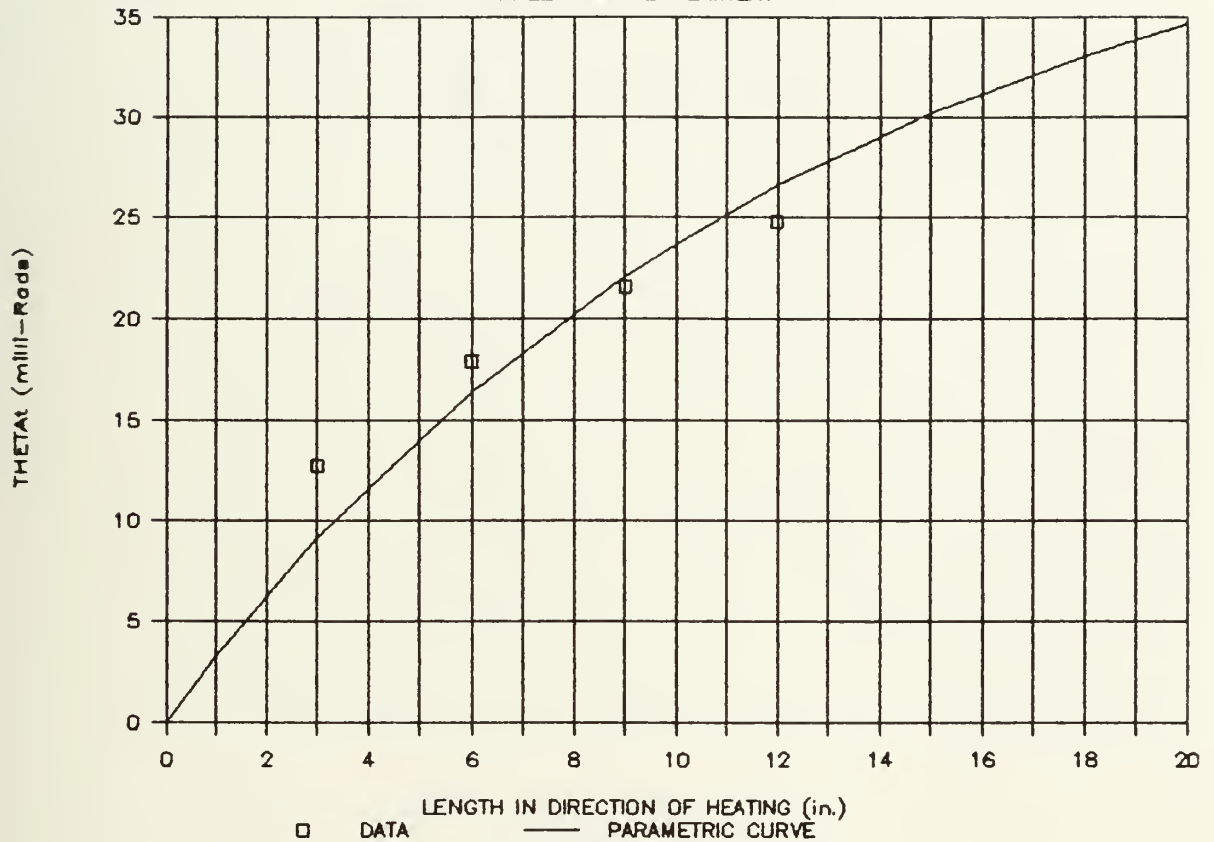
The graphical results of fitting a curve of the form,

$$\theta_t(L) = A(1 - e^{-BL}),$$

to the plate length vs. bending data for flame and laser heating are contained in this appendix. The parametric values for each case studied have been summarized in Table 5.1.

PARAMETRIC STUDY

PRELIMINARY EXPERIMENT

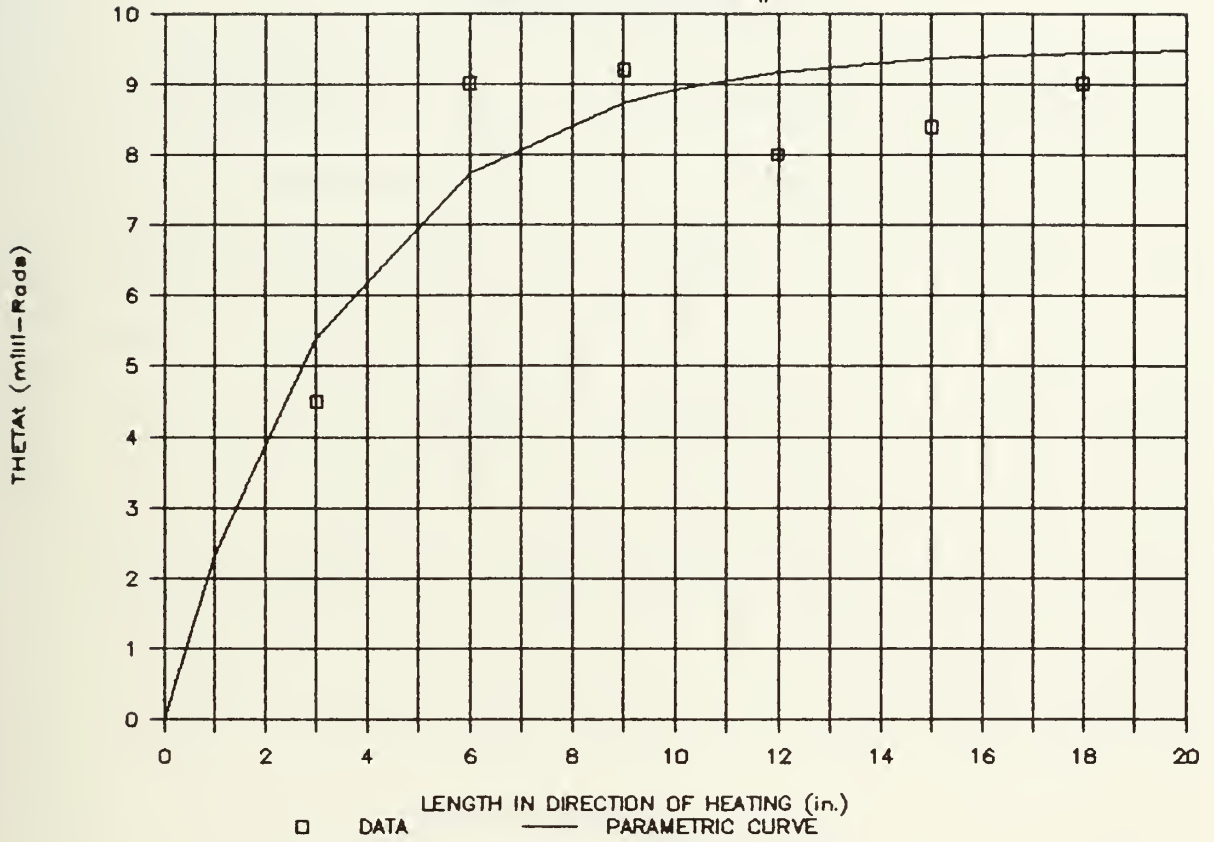


$$A=43.90 \quad B=0.078$$

FIGURE A.1 FLAME HEATING 3/8" PLATE-- PRELIMINARY EXPERIMENT

PARAMETRIC STUDY

FOLLOW-ON EXPERIMENT # 1

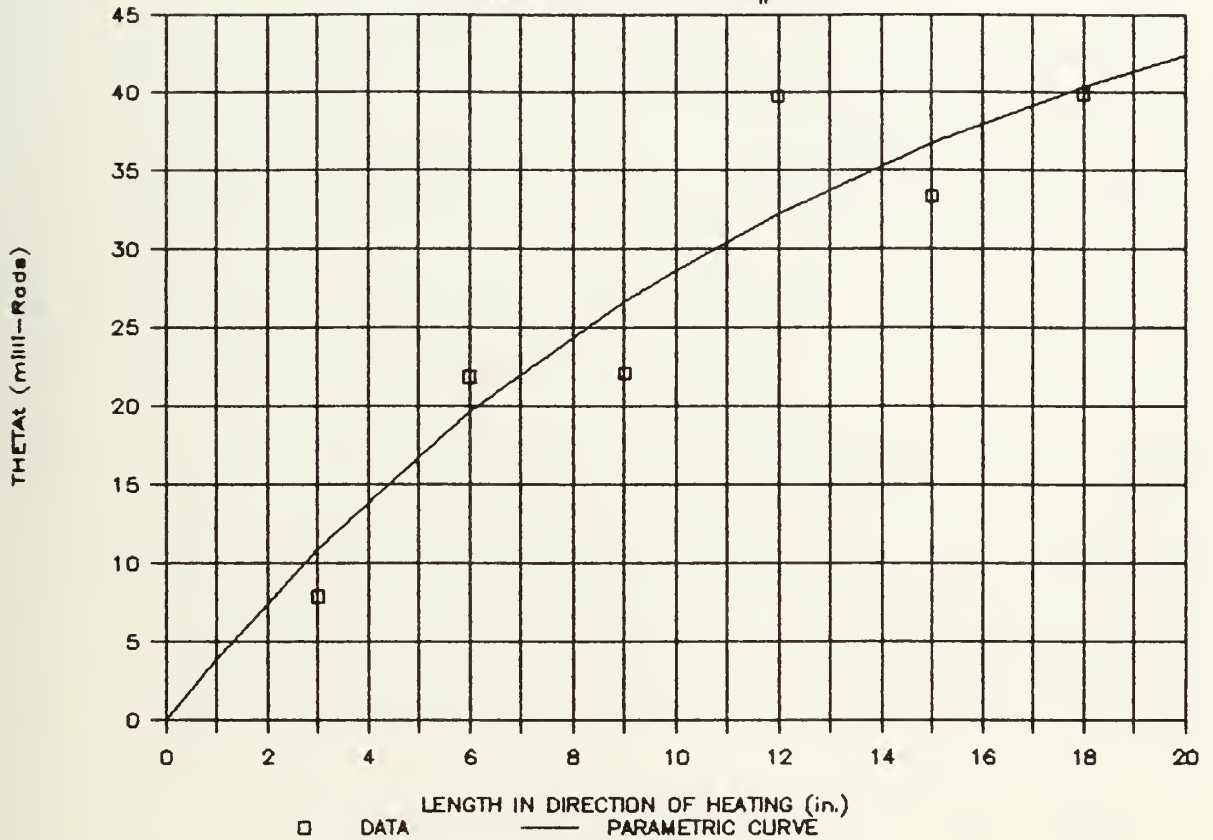


$$A=9.50 \quad B=0.280$$

FIGURE A.2 FLAME HEATING 3/8" PLATE-- FIRST FOLLOW-ON EXPERIMENT

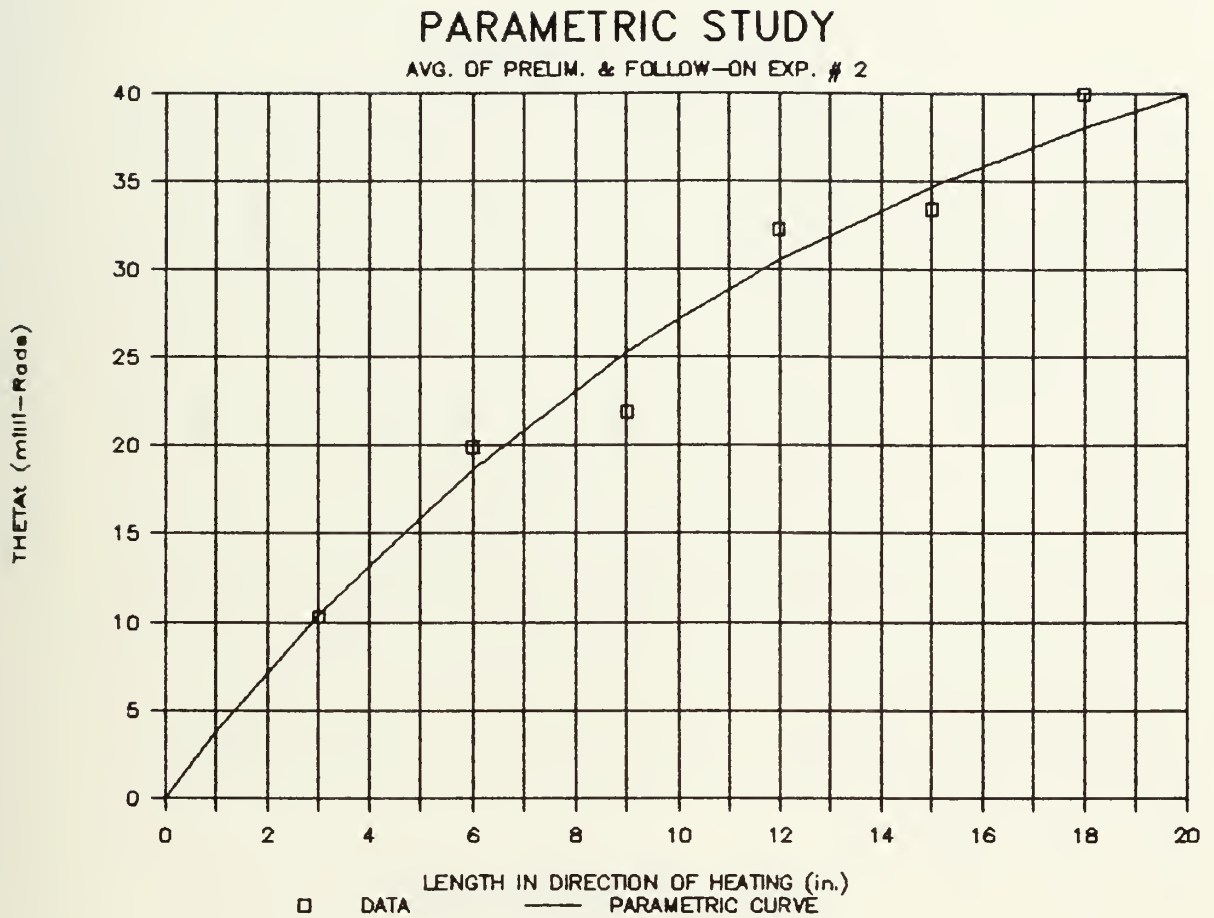
PARAMETRIC STUDY

FOLLOW-ON EXPERIMENT # 2



$$A=55.00 \quad B=0.074$$

FIGURE A.3 FLAME HEATING 3/8" PLATE-- SECOND FOLLOW-ON EXPERIMENT

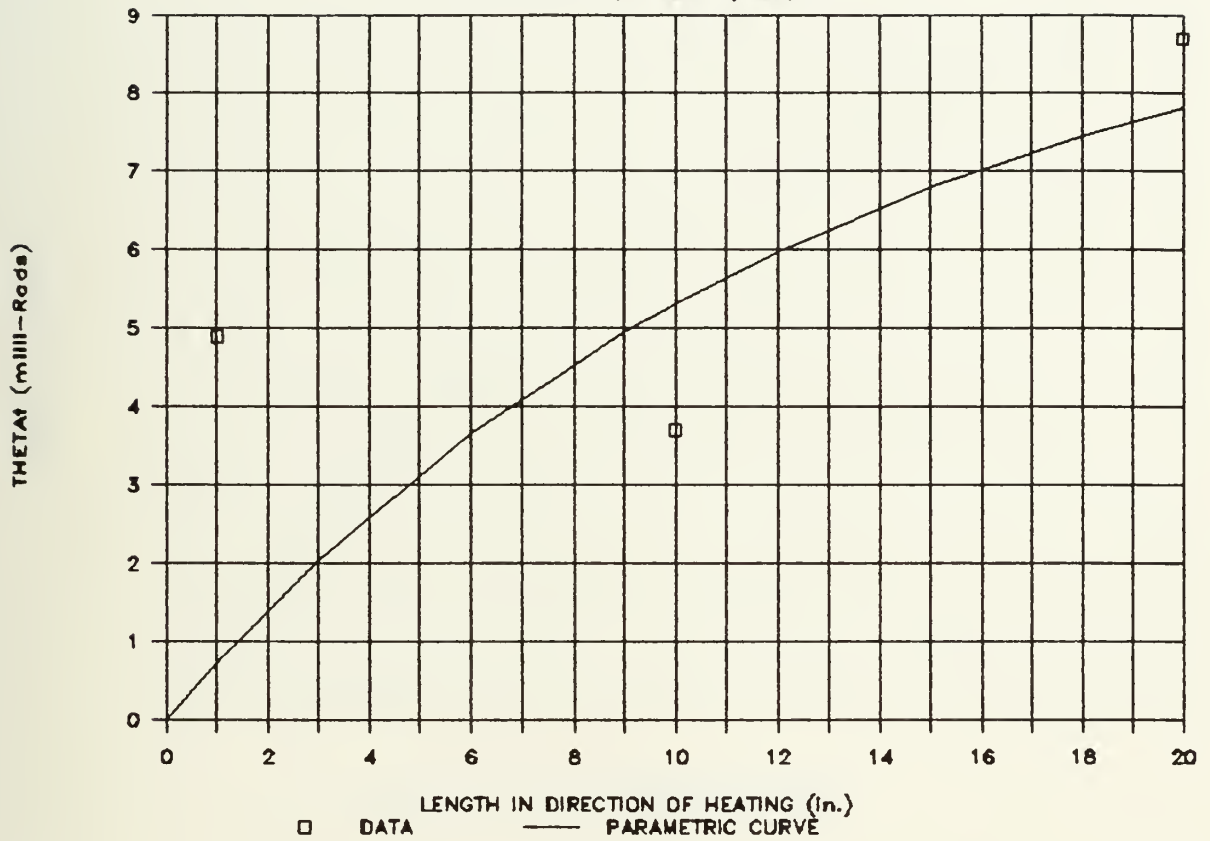


$$A=51.70 \quad B=0.075$$

FIGURE A.4 FLAME HEATING 3/8" PLATE-- AVERAGE OF PRELIMINARY & SECOND FOLLOW-ON EXPERIMENT

PARAMETRIC STUDY

LASER DATA: $P/\sqrt{V} = 2.0$, $t=3/8$

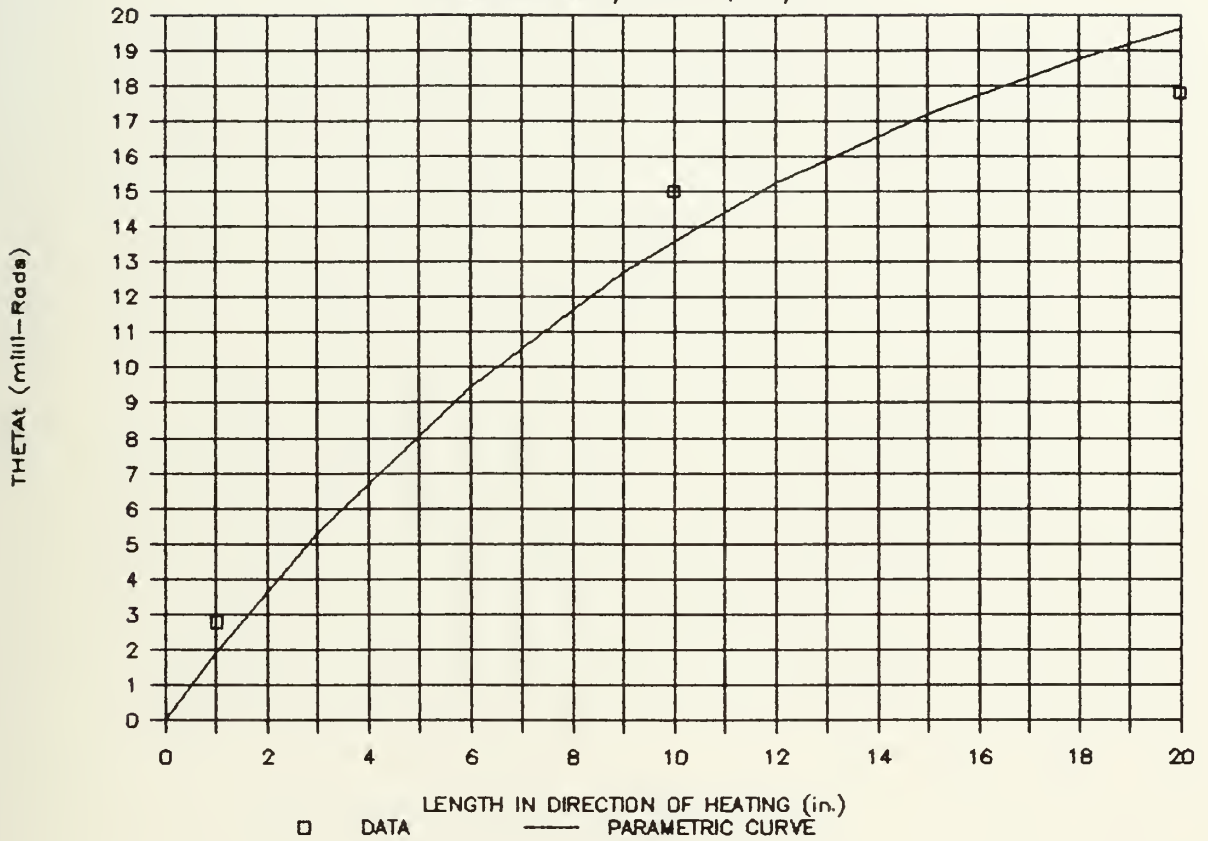


A=10.00 B=0.076

FIGURE A.5 LASER HEATING 3/8" PLATE-- # 1

PARAMETRIC STUDY

LASER DATA: P/W = 2.5, t=3/8

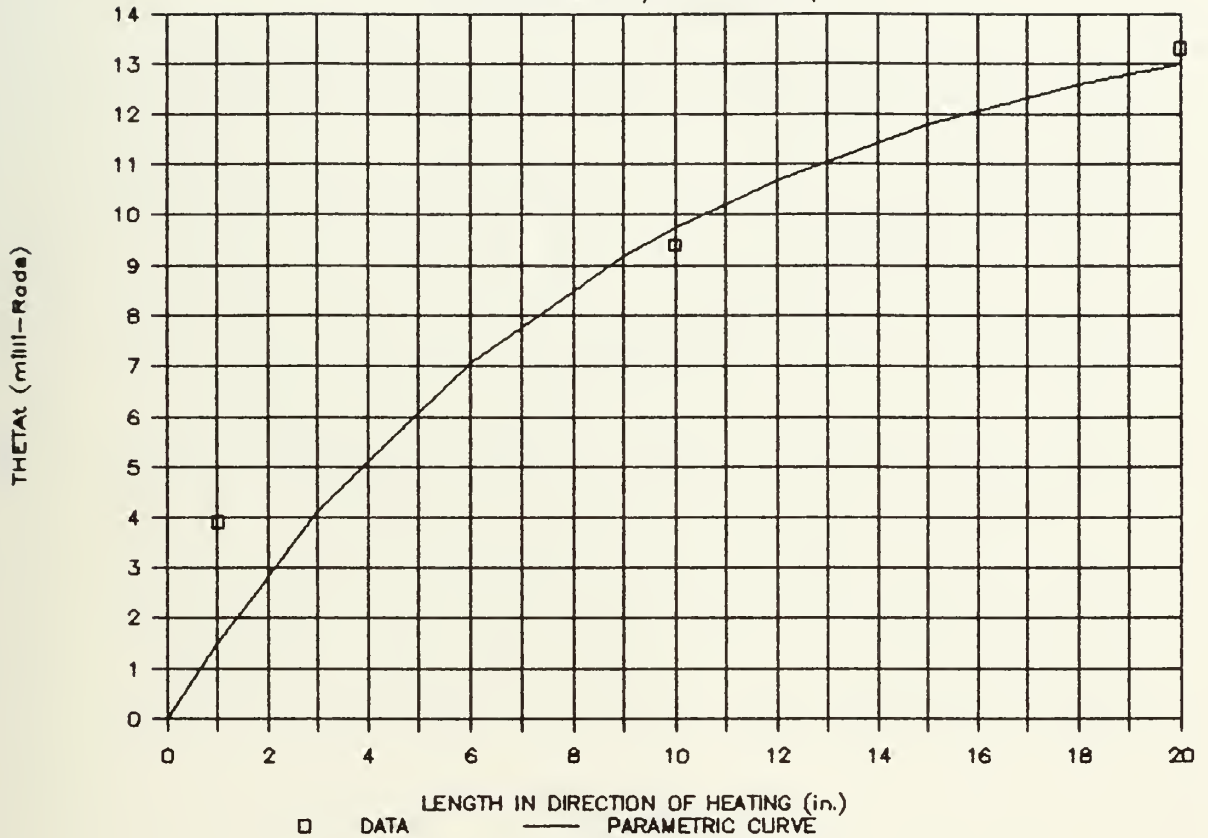


$$A=24.30 \quad B=0.082$$

FIGURE A.6 LASER HEATING 3/8" PLATE-- # 2

PARAMETRIC STUDY

LASER DATA: AVG. $P/\sqrt{v} = 2.3$, $t=3/8$

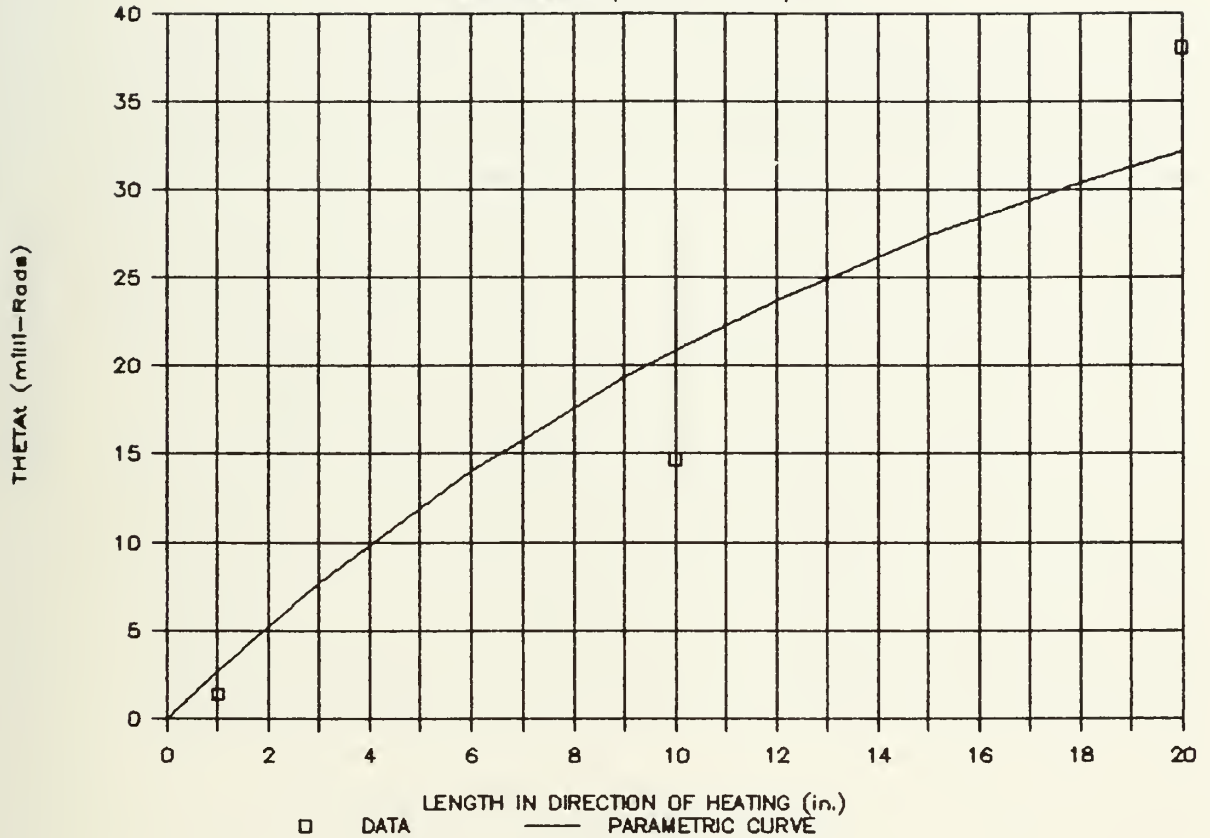


$$A=14.60 \quad B=0.110$$

FIGURE A.7 LASER HEATING 3/8" PLATE-- AVERAGE OF # 1 & # 2

PARAMETRIC STUDY

LASER DATA: $P/\sqrt{W} = 1.8$, $t=1/2$

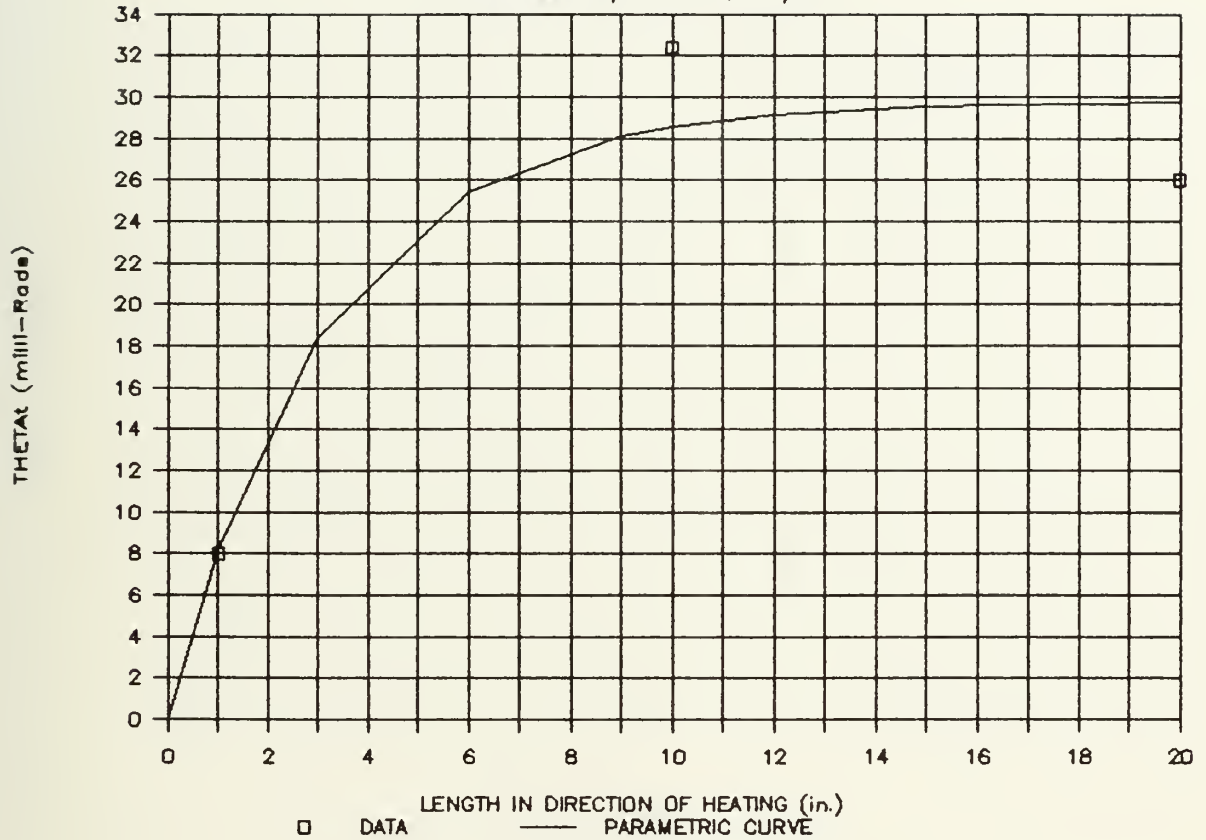


$$A=45.20 \quad B=0.062$$

FIGURE A.8 LASER HEATING 1/2" PLATE-- # 3

PARAMETRIC STUDY

LASER DATA: $P/\sqrt{W} = 2.5$, $t = 1/2$

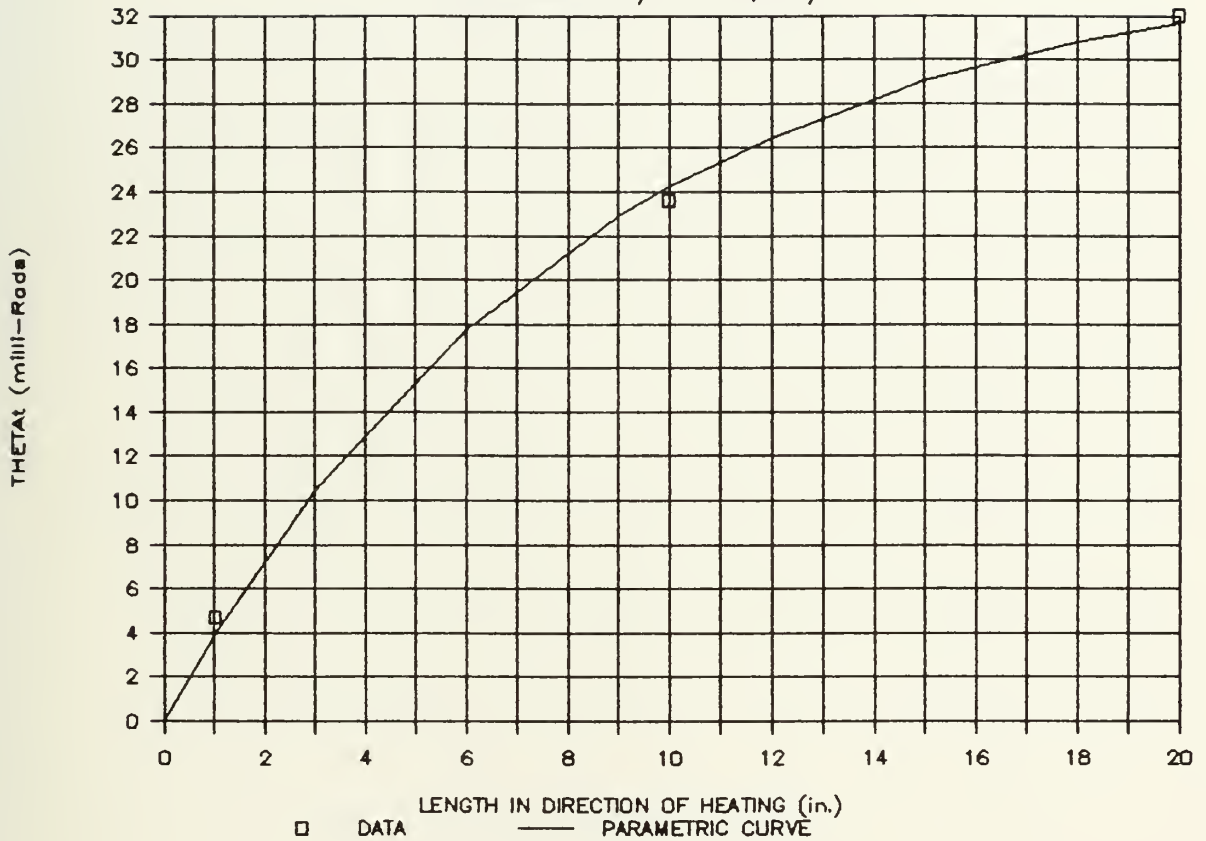


$$A=29.80 \quad B=0.320$$

FIGURE A.9 LASER HEATING 1/2" PLATE-- # 4

PARAMETRIC STUDY

LASER DATA: AVG. $P/\sqrt{v} = 2.1$, $t=1/2$

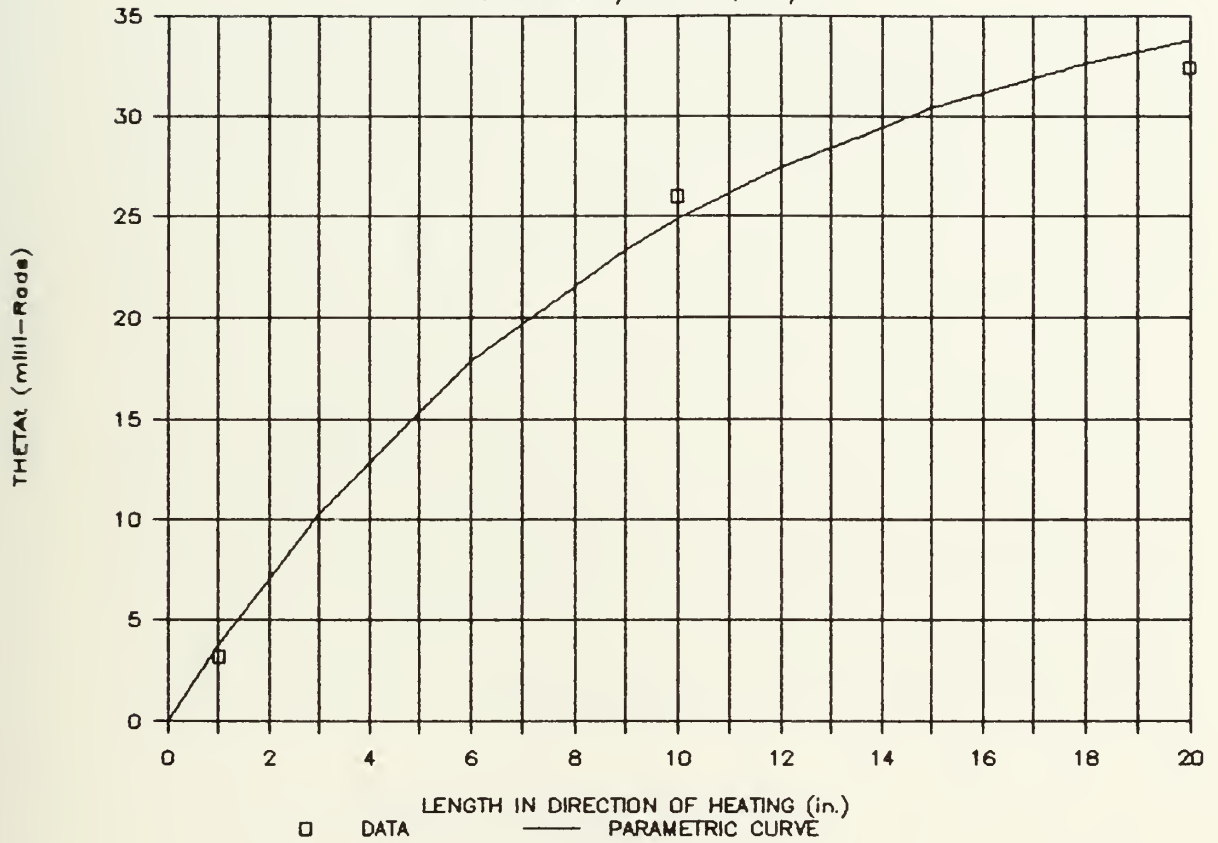


$$A=35.00 \quad B=0.118$$

FIGURE A.10 LASER HEATING 1/2" PLATE-- AVERAGE OF # 3 & # 4

PARAMETRIC STUDY

LASER DATA: $P/\sqrt{V} = 3.0$, $t=5/8$

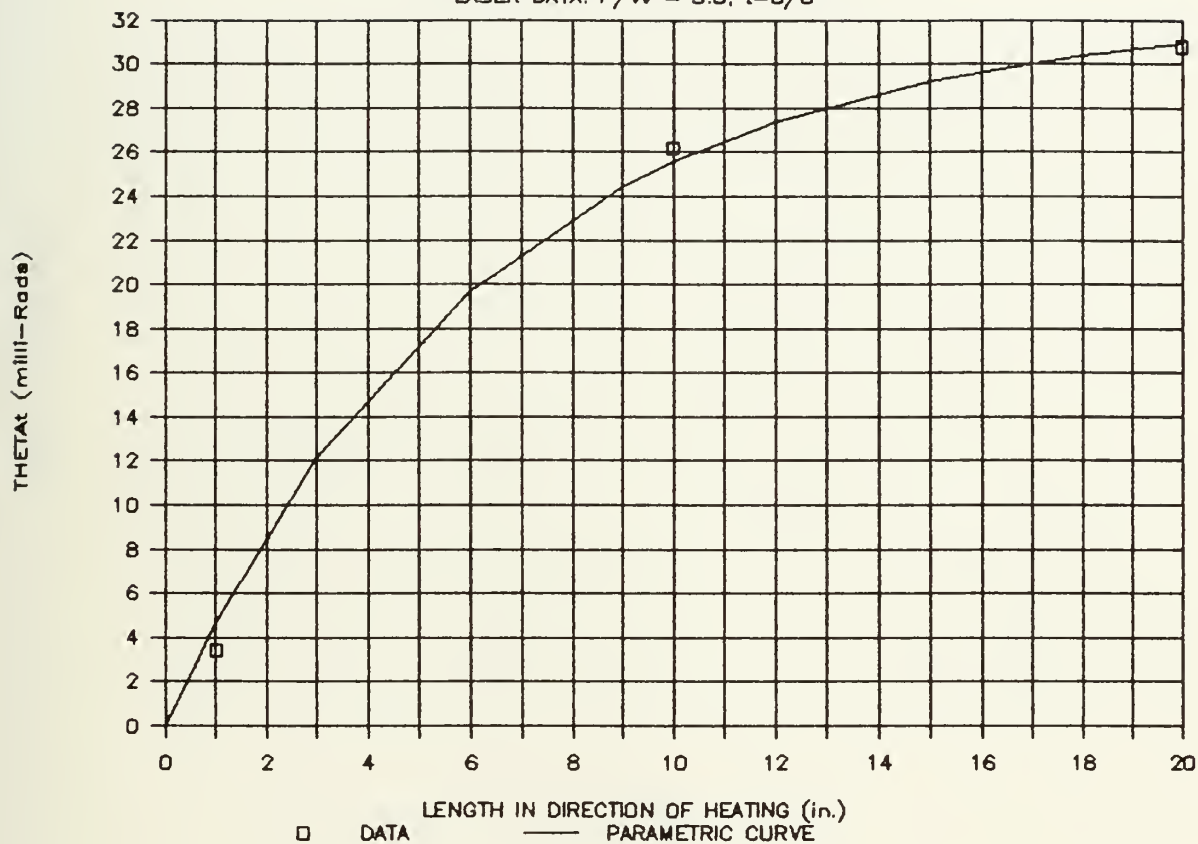


$$A=38.70 \quad B=0.103$$

FIGURE A.11 LASER HEATING 5/8" PLATE-- # 5

PARAMETRIC STUDY

LASER DATA: $P/W = 3.5$, $t = 5/8$

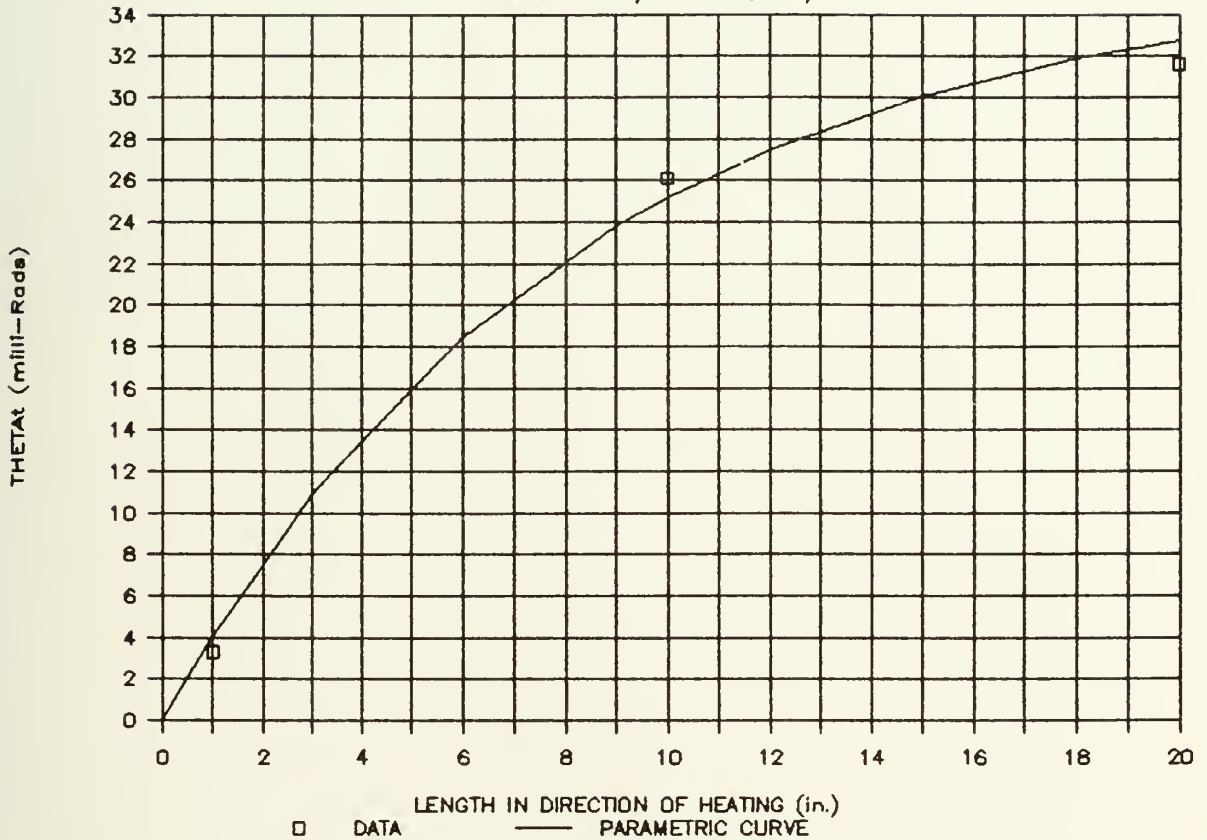


$$A=32.30 \quad B=0.157$$

FIGURE A.12 LASER HEATING 5/8" PLATE-- # 6

PARAMETRIC STUDY

LASER DATA: AVG. $P/\sqrt{V} = 3.3$, $t=5/8$



$$A=36.03 \quad B=0.121$$

FIGURE A.13 LASER HEATING 5/8" PLATE-- AVERAGE OF # 5 & # 6

DUDLEY KNOT LIBRARY
MILLER SCHOOL
MONTEREY, CALIFORNIA 93943-5002

Thesis

M27767 Malaret

c.1 Mechanisms in thermal
mechanical forming of
plates.

Thesis

M27767 Malaret

c.1 Mechanisms in thermal
mechanical forming of
plates.

thesM27767

Mechanisms in thermal mechanical forming



3 2768 000 75120 0

DUDLEY KNOX LIBRARY

c.1